UNCLASSIFIED

AD NUMBER
AD109766
CLASSIFICATION CHANGES
TO: **UNCLASSIFIED**
FROM: **CONFIDENTIAL**
LIMITATION CHANGES
TO: **Approved for public release; distribution is unlimited.**
FROM: **Distribution authorized to U.S. Gov't. agencies and their contractors; Administrative/Operational Use; 20 DEC 1950. Other requests shall be referred to Office of Naval Research, Arlington, VA 22203.**
AUTHORITY
ONR ltr 26 Oct 1977 ; ONR ltr 26 Oct 1977

THIS PAGE IS UNCLASSIFIED

CONFIDENTIAL

109766

1-229

M[illegible]NELL AIRCRAFT CORPORATION

[illegible]IBERT-ST. LOUIS MUNICIPAL AIRPORT

DETAILED FINAL REPORT OF RESEARCH ON
HIGH-SPEED ROTARY-FIXED WING AIRCRAFT

VOLUME IV

SAMPLE AIRCRAFT PERFORMANCE DATA

OFFICE OF NAVAL RESEARCH, AMPHIBIOUS BRANCH
PROJECT NR 250-001 CONTRACT N[illegible]

Report 1904-A Serial 16

20 December 1950

56AA 58584

Enclosure (5) to
MAC Letter 2136-701-1756

CONFIDENTIAL

MAC 273 (REV. 2-24-50)

CONFIDENTIAL

REPORT 1904-A

DATE 20 December 1950

REVISED

McDONNELL Aircraft Corporation

ST. LOUIS 3, MISSOURI

DETAILED FINAL REPORT OF RESEARCH ON HIGH SPEED ROTARY-FIXED WING AIRCRAFT

VOLUME IV

SAMPLE AIRCRAFT PERFORMANCE DATA

SUBMITTED UNDER Contract N9onr-84901 to the Office of Naval Research, Amphibious Branch, Project NR 250-001

PREPARED BY R.C. Snyder A.N. Hock R.C. Snyder A.N. Hook

APPROVED BY K. H. Hohenemser K. H. Hohenemser

APPROVED BY

APPROVED BY C. H. Hurkamp C. H. Hurkamp

CONFIDENTIAL

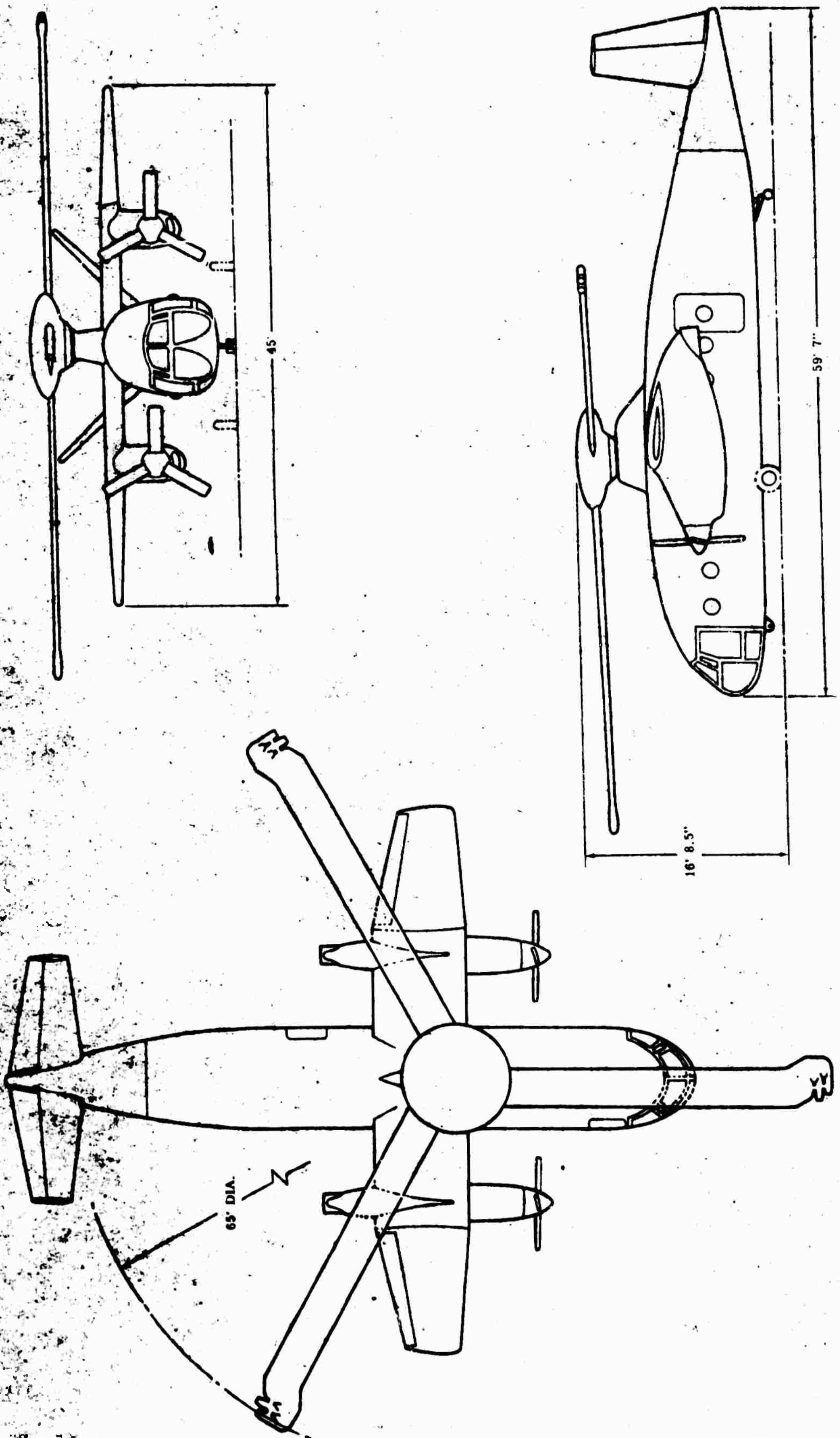

GENERAL ARRANGEMENT - MODEL 78

20 December 1950

CONFIDENTIAL

Report 1904
Model 78

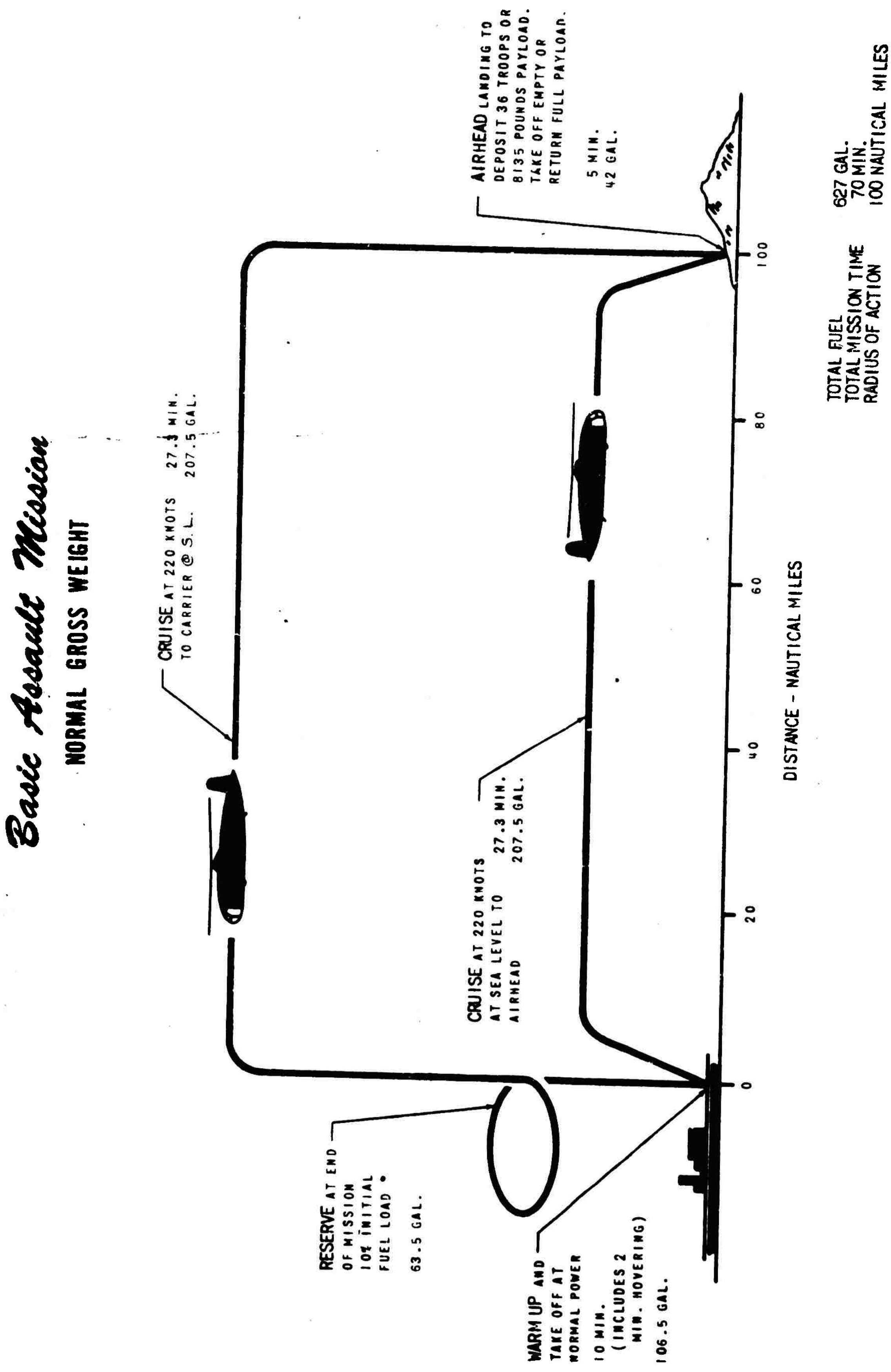

CONFIDENTIAL

MAC 231 (REV. [illegible] 49)

DATE 29 [illegible]

REVISED

REVISED

McDONNELL *Aircraft Corporation*

ST. LOUIS 3, MISSOURI

CONFIDENTIAL

PAGE 1

REPORT [illegible]

MODEL [illegible]

[illegible]

CONFIDENTIAL

1. SUMMARY

The preliminary estimated performance data characteristics are presented for a rotorcraft of advanced design that fulfills or exceeds the specified requirements for an assault helicopter. This helicopter, designated the Model 78, is propelled by a rotor for take-off, hovering, and slow translational flight, and by propellers for cruise and high-speed flight. For rotor-propelled flight, a pressure-jet rotor system and conventional helicopter controls are utilized. For high-speed flight, the major portion of the aircraft weight is supported by a small fixed-wing surface with the lightly loaded rotor in low-pitch autorotation. Two gas turbine-driven propellers and conventional airplane controls provide propulsion and control.

The vertical and high-speed flight characteristics and high payload of Model 78 are readily adapted to an assault mission. At the maximum level flight speed of 240 knots and an 8135-pound payload (36 troops), thirty-three troops per hour per aircraft can be transported to an airhead, as compared to the 9.7 troops per hour per aircraft just meeting the assault specifications. Therefore, on the first wave, the Model 78 is capable of performing the work of 1.8 aircraft which just meet the assault specification, or on a shuttle basis, is the equivalent of 3.4 such aircraft.

All performance estimates are based upon proven methods of analysis developed by the NACA, or upon wind tunnel model test data obtained in a twenty-month research program under contract to the Office of Naval Research. Much of these test data have shown substantial agreement with data from previous test programs of the NACA and with McDonnell theoretical analyses.

2. INTRODUCTION

The McDonnell Aircraft Corporation presents herewith the preliminary aerodynamic performance estimates for a rotorcraft of advanced design. This aircraft, designated the Model 78, has the cruise speed of an airplane, the lifting capacity of a jet rotor and the ability to land either troops or cargo at any selected point. The design principle is based upon the finding that lifting rotors, when not required to deliver the entire lifting or propulsive force of the aircraft, may advance at far higher speeds than heretofore considered possible. This principle has been confirmed as a result of twenty months of research conducted under contract to the Office of Naval Research. Rotor lift, drag, blade motions, blade stresses, wing interference, aircraft stability, and many other details have been analyzed and tested through a wide range of variables.

The Model 78 incorporates a single lifting rotor with pressure-jet drive, a relatively small fixed wing to unload the rotor at high speeds, a conventional empennage for aircraft stability, a twin-engine installation driving variable-pitch propellers and two axial flow compressors for rotor propulsion, and side-by-side seating for pilot and copilot. The twin-engine design using available gas turbines and compressors (Allison 501 and Westinghouse 19-XB respectively) offers reliability and greatly improved performance over that of conventional helicopters. Since the rotor autorotates in forward flight and rotor power is required only for short periods of hovering and acceleration, it is possible to use a jet drive without appreciable penalty from its relatively high fuel consumption. Of the jet rotor drives available, the pressure-jet rotor is the most suitable because of its lower fuel consumption, easier starting and high power, its high

lifting capacity and its ability to fulfill the autorotational requirements at high forward speeds.

For hovering and slow forward flight, the aircraft is flown by rotor propulsion utilizing the pressure-jet power system derived from turbine-driven compressors and conventional single rotor control (i.e., vertical control by collective pitch variation and transverse control by cyclic pitch variation.) For high-speed flight, in which the major portion of the weight is supported by a fixed wing and in which the lightly loaded rotor is autorotating, propulsion is obtained from two gas turbine-driven propellers and control is by conventional airplane aileron-elevator-rudder systems. The transition from rotor-driven to propeller-driven flight is performed at nearly constant altitude by shifting from pressure-jet power to propeller power with the intermediate power being supplied by the residual rotor kinetic energy and a change in velocity kinetic energy.

Although Model 78 is designed to presently-considered practical values of blade tip speed and maximum advance ratio in order to guarantee its immediate usefulness in military operation, rotor model tests conducted up to an advance ratio of 2.5 have shown that, even for a Mach number of the advancing blade less than .85, flight speeds over 350 knots may be attained in the future. The most surprising result of these model tests, confirmed by theoretical studies, was the increase of aerodynamic efficiency with increasing advance ratio. A lift to drag ratio of the autorotating model rotor (excluding hub) of 11.5 was measured at an advance ratio of 2.5. This indicates full-scale lift to drag ratios of the same order of magnitude as those for a fixed wing. A number of problems pertaining to rotor control, blade motions and blade stresses have to be studied prior to the

utilization of tip speeds and advance ratios very much in excess of these used in the normal operation of Model 78.

The preliminary performance estimates for the Model 78 are based upon wind tunnel model test data, obtained in a research program sponsored by the Office of Naval Research, and in the conventional helicopter or rotor propulsion advance ratio range, upon proven methods of analysis.

3. [illegible] PERFORMANCE [illegible]

3.1 Summary Performance Table and Figures

Take-off weight	30,[illegible]00 pounds
Fuel	3760 pounds
Payload	8135 pounds
Engine power (normal rating)*	3870/14000 Bhp/rpm
Disc loading (W/A)	[illegible].04 lbs./sq.ft.
Power loading	7.75 lbs./hp
Maximum speed - sea level	240 knots
Rate of climb - sea level	
Rotor propulsion	[illegible]120 ft./min.
Propeller propulsion	18[illegible]0 ft./min.
Time to 5000 feet	
Rotor propulsion	1.70 min.
Propeller propulsion	2.[illegible] min.
Time to 10,000 feet	
Rotor propulsion	4.18 min.
Propeller propulsion	6.51 min.
Vertical rate of climb - sea level . .	3040 ft./min.
Absolute hovering ceiling . . . . (stall limitation)	10,000 feet
Combat radius/Average velocity	100 n.mi./220 knots
Maximum endurance/Average velocity . .	1.28 hrs./2[illegible]0 knots
Ferry range (1880 gal. fuel)	776 nautical miles

* Power available, considering losses

FIGURE - 1

Level Flight Performance

HORSEPOWER REQUIRED VS VELOCITY

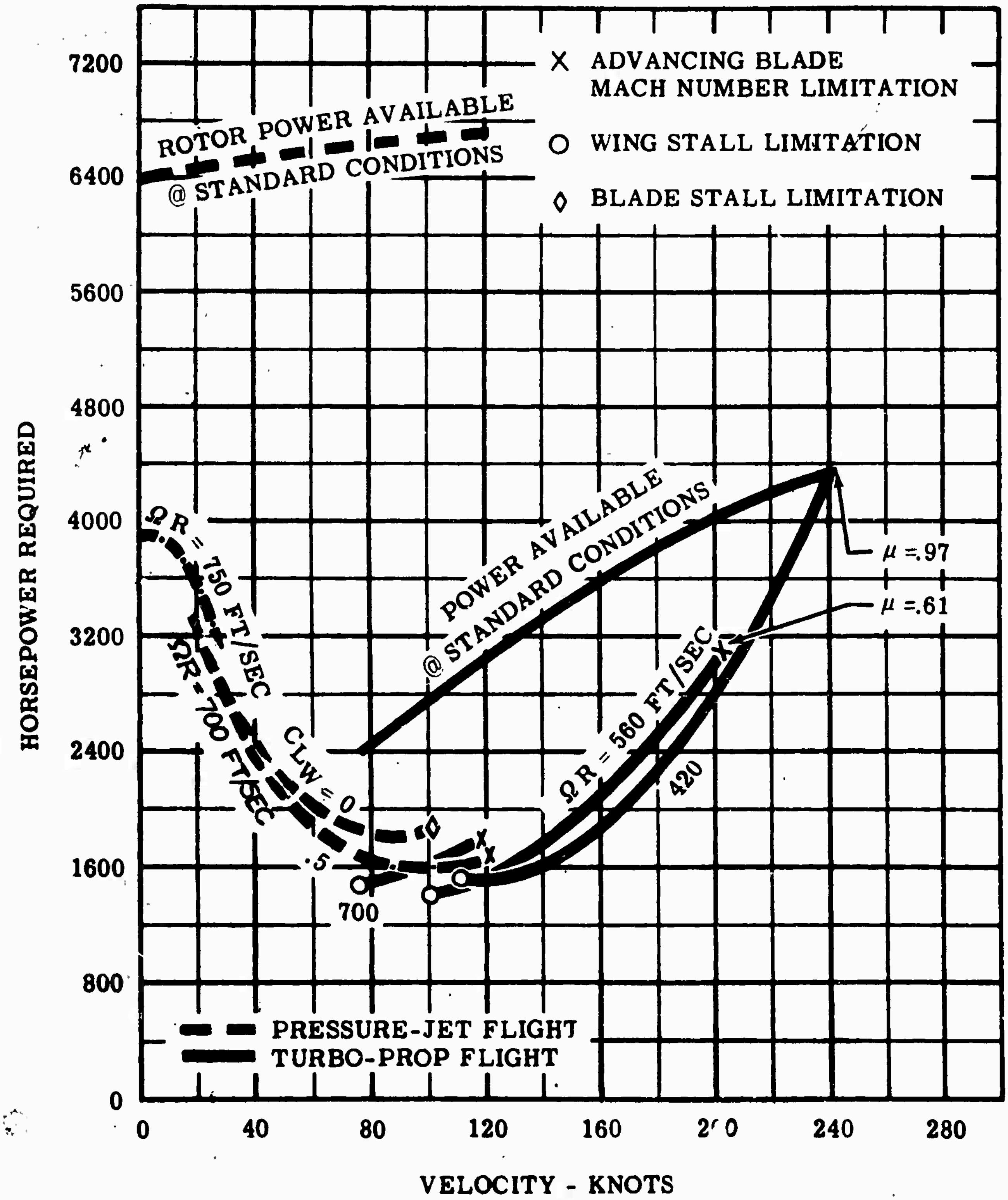

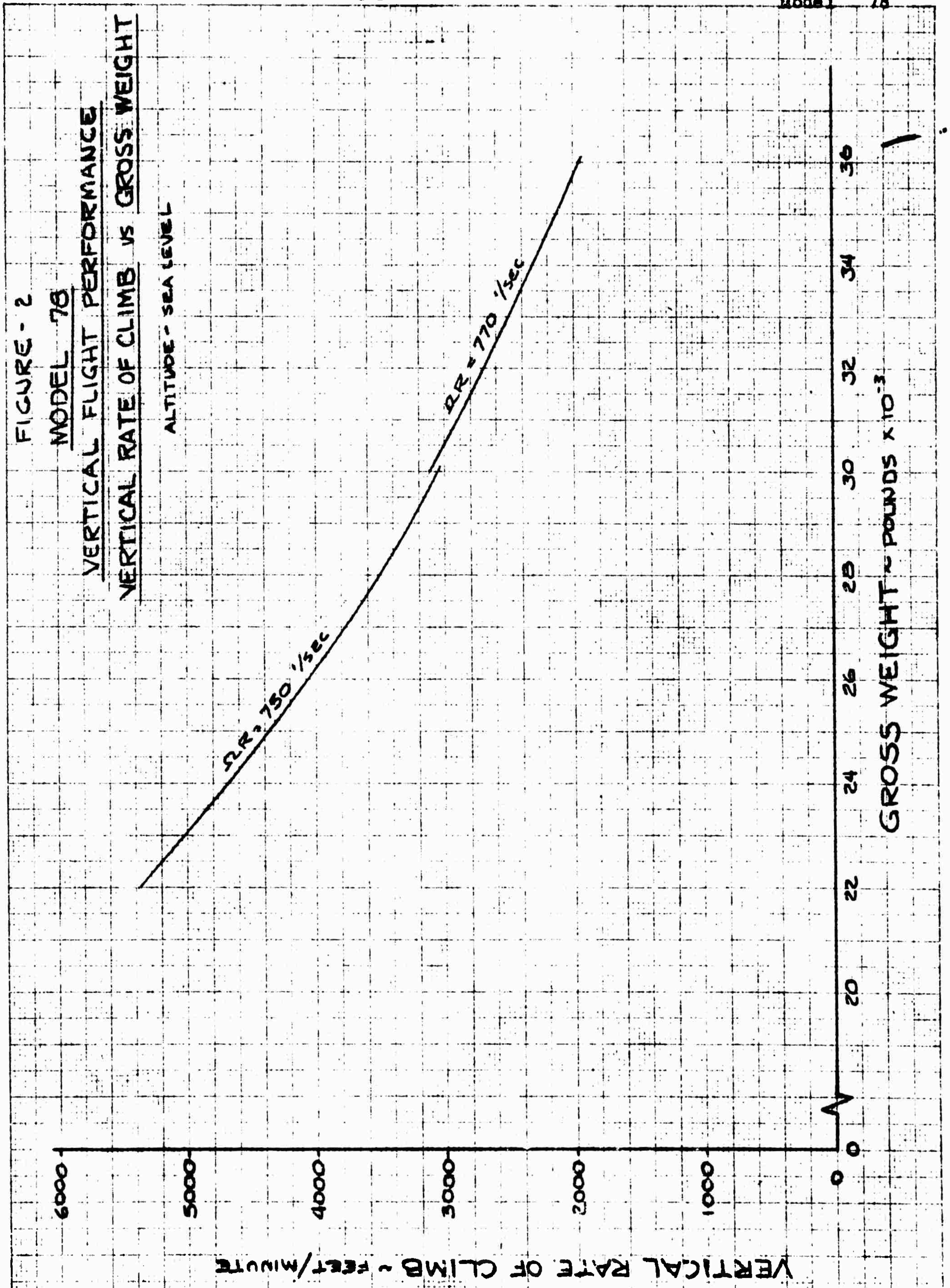
FIGURE - 2
MODEL 78
VERTICAL FLIGHT PERFORMANCE
VERTICAL RATE OF CLIMB VS GROSS WEIGHT
ALTITUDE - SEA LEVEL
ΩR = 750 '/SEC
ΩR = 770 '/SEC
GROSS WEIGHT ~ POUNDS x 10⁻³
0
20
22
24
26
28
30
32
34
36
VERTICAL RATE OF CLIMB ~ FEET/MINUTE
0
1000
2000
3000
4000
5000
6000

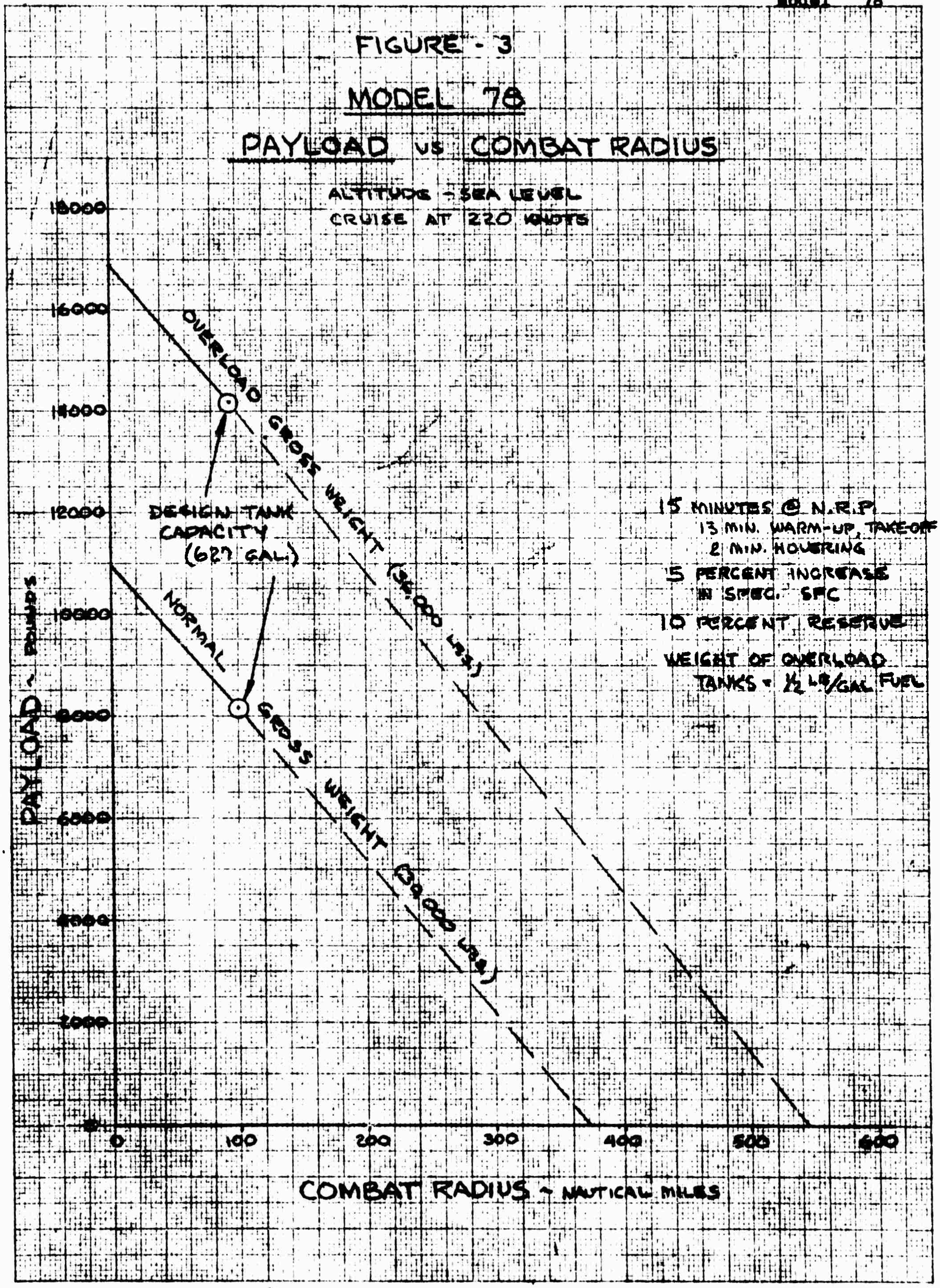
FIGURE - 3
MODEL 78
PAYLOAD vs COMBAT RADIUS
ALTITUDE - SEA LEVEL
CRUISE AT 220 KNOTS
OVERLOAD GROSS WEIGHT (36,000 LBS.)
NORMAL GROSS WEIGHT (33,000 LBS.)
DESIGN TANK CAPACITY (627 GAL.)
15 MINUTES @ N.R.P.
13 MIN. WARM-UP, TAKE-OFF
2 MIN. HOVERING
5 PERCENT INCREASE IN SPEC. SFC
10 PERCENT RESERVE
WEIGHT OF OVERLOAD TANKS = 1/2 LB/GAL FUEL
PAYLOAD ~ POUNDS
18000
16000
14000
12000
10000
8000
6000
4000
2000
0
0
100
200
300
400
500
600
COMBAT RADIUS ~ NAUTICAL MILES

FIGURE - 4

MODEL 78

LEVEL FLIGHT PERFORMANCE

AVERAGE SPEED vs COMBAT RADIUS

NORMAL GROSS WEIGHT
ALTITUDE - SEA LEVEL

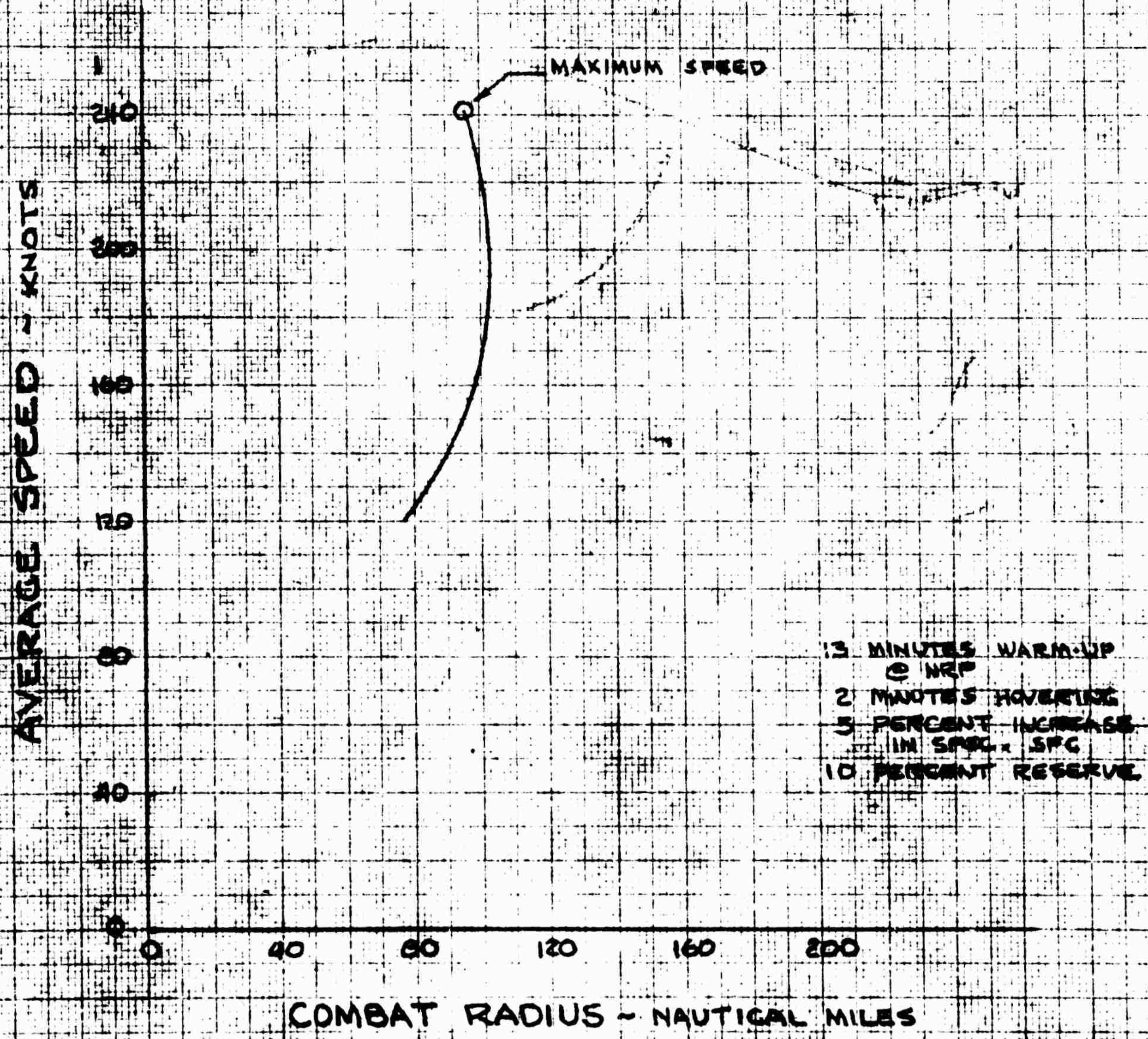

4. DISCUSSION

The principle of a combined rotary-fixed wing aircraft was reduced to practice in the early days of the autogyro, and an extensive flight test program has been conducted with such aircraft by the NACA (references 9.11 and 9.12). This program included conditions up to an advance ratio of the lifting rotor of .7 and up to a load on the fixed wing of 35% of the total aircraft weight. The aircraft tested by the NACA was controlled by conventional aileron, elevator, and rudder controls with no means provided to change the relative attitude of wing and lifting rotor or the blade pitch angle in flight. The main conclusions from these tests were that a wide variation of rotor speed as a function of airspeed may be obtained by suitable adjustments of the relative wing and rotor attitude (which were made on the ground during the test program) and that the interference of the wing on the lifting rotor is negligible in the tested range.

As compared to this early version of rotary-fixed wing aircraft, model 78 incorporates the following additional features: a rotor attitude control, longitudinally and laterally; a collective blade pitch control; and jet rotor drive for vertical take-off and forward acceleration up to 118 knots. In rotor propelled, or pressure-jet flight, which is possible between zero and 118 knots, the aircraft is controlled by the longitudinal and lateral rotor attitude control with the fixed surface controls relatively ineffective. In propeller propulsion, or turbo-prop flight, which is possible between 30 and the limit dive speed of 300 knots, the aircraft is controlled by the fixed surface controls. The rotor lateral attitude control is still connected to the control stick, though relatively ineffective, while the rotor longitudinal attitude control is disconnected from

the control stick and an automatic rotor attitude control is incorporated to achieve rotor speed stability.

The design features of the model are selected to insure immediate usefulness in military operation. Available power plants, compressors, and practical limits on the rotor advance ratio, rotor diameter, etc., are used to guarantee such operation. Although the gas turbine has, when operating at the lower altitudes, part throttle, and on heavy Summer days, a higher fuel consumption than a reciprocating engine, the saving in weight and in aerodynamic drag by far offsets these disadvantages for the relatively short range that is required for an assault aircraft. Gas turbine development to be expected during the prototype design stage of this aircraft should further enhance their selection.

5. TABULATED DATA

5.1 Notation and Symbols -

a	=	Lift curve slope
AR	=	Aspect ratio
A	=	Area, square feet
b_n	=	Number of blades
b	=	Span, feet
c	=	Mean chord, feet
C_T	=	Rotor thrust coefficient $\frac{T}{\rho \pi R^2 (\Omega R)^2}$
C_T/σ	=	Aerodynamic blade loading
C_{L_R}	=	Rotor lift coefficient $\frac{L_R}{\rho/2 \, \pi R^2 V^2}$
C_{L_W}	=	Fixed wing lift coefficient $\frac{L_W}{\rho/2 \, A_W V^2}$
C_Q	=	Rotor torque coefficient $\frac{Q}{\rho \pi R^2 (\Omega R)^2 R}$
D/L	=	Equivalent drag-lift ratio
f	=	Parasite drag area, square feet
F	=	Pressure-jet thrust, pounds
K_V	=	Ratio $\frac{\text{Excess Power}}{\text{Effective vertical climb power}}$
L	=	Total lift force, pounds
L_R	=	Rotor lift force, pounds
L_W	=	Fixed wing lift force, pounds
L/D	=	Lift-drag ratio

Q = Rotor torque, foot-pounds

q = Dynamic pressure, pounds/square foot

R = Rotor radius, feet

R/C = Maximum rate of climb, feet/minute

T = Rotor thrust, pounds

T/F = Hovering merit factor

v_i = Rotor induced velocity, feet/second

V = Flight path velocity, feet/second

V_v = Vertical rate of climb, feet/second

μ = Advance ratio, $\frac{V}{\Omega R}$

Ω = Rotor angular velocity, radians/second

ρ = Air density, slugs/cubic feet

σ = Rotor solidity, $\frac{b_r C_r}{R}$

θ = Rotor blade angle, degrees

$\alpha_{(Tip)(270)}$ = Retreating blade tip angle of attack, degrees

Subscripts

i = Induced

J = Tip jet

o = Profile

P = Parasite

R = Rotor

W = Fixed-wing

5.2 Dimensional Data -

5.2.1 Fixed Wing

Span, inches	540
Chord, inches: root	97.75
tip	57
MAC	90
Projected area, sq.ft.	332
Airfoil section - root	23018
tip	23012
Incidence, degrees	3
Effective aspect ratio	6.1
Aileron area, sq.ft.	21.50
Split-flap area, sq.ft.	18.00

5.2.2 Rotors

Number of rotors	1
Number of blades per rotor	3
Rotor diameter, feet	65
Rotor disc area, sq.ft.	3320
Disc loading, lbs./ft.^{2}	9.04
Rotor solidity	.09
Blade chord, inches	37
Blade twist, degrees	0
Blade airfoil section	NACA 23015
Rotor tip speed, ft./sec. -	
Hovering	750
Helicopter forward flight	750, 700
Propeller forward flight	700, 560, 420

5.2.3 Empennage (V-type)

Airfoil section - root	NACA 0015
tip	NACA 0009
Effective aspect ratio	[illegible].65
Dihedral, degrees	45
Normal incidence, degrees	0
Mean aerodynamic chord, inches	[illegible]2.25
Total area, sq.ft.	142.0
Control surface area, sq.ft.	44.0

5.2.4 Propellers

Number of propellers	2
Number of blades per propeller	3
Manufacturer	Aero Products
Model designation	A 632F
Propeller diameter, feet	10
Activity factor	4[illegible]0
Propeller gear ratio	7.95:1
Propeller speed, rpm	1760

5.3 Weight Data

5.3.1 Normal gross weight, pounds	30,000
Weight empty	1[illegible],[illegible]54
Useful load	1[illegible],046
Payload	[illegible],135

5.3.2 Maximum T.O. weight, pounds 30,000

Weight empty 16,954

Useful load 13,046

Payload 14,135

5.4 Power Plant Data *

5.4.1 Engine Data

Number of engines 2

Manufacturer . . . . Allison Division, General Motors

Model designation . . . . Allison Model 501 power section

Engine ratings -
Specification normal rating 2235/14000
Performance normal rating ** 1935/14000

5.4.2 Compressor Data

Manufacturer . . . . Westinghouse

Model designation 19XB

5.4.3 Pressure-Jet Data

Manufacturer . . . . McDonnell Aircraft Corporation

* For more complete Power Plant data, see reference 9.7.

** Includes losses for inlets, ducts, etc., see reference 9.8.

6. AERODYNAMIC DATA

6.1 Parasite drag estimate - For estimating parasite drag power losses, a breakdown of the component parasite drag areas is made. The following tables of component parasite drag areas were prepared to cover the requirements of the performance estimate. The component drag coefficients were obtained from reference 9.5. Note that the wing is not considered in Table I, since the drag effect of the wing in forward flight is included in the L/D of the wing. Also, the hub effect is treated as a separate component in the rotor-powered flight performance, and for turbo-prop flight, the hub drag is contained in the L/D for the rotor.

TABLE I

Component	Area	C_D	f(sq.ft.)
Fuselage	68.5	.11	7.54
Pylon	26.5	.016	.42
Nacelles	29.5	.10	2.95
Empennage	120.0	.012	1.44
Landing gear (retracted)	-	-	.35
Interference (10% assumed)	-	-	1.30
		Total	14.00 *
Hub (based on disc area, C_D from model test data)		.0013	4.32
		Total	18.32 **

* Turbo-prop flight (wing drag, induced and profile, included in L/D wing; hub drag included in L/D of rotor).

** Powered rotor flight (wing drag, induced and profile, included in L/D wing).

TABLE II

Parasite Drag Estimate (Vertical flight) *

Component	Area	C_D	f(sq.ft.)
Fuselage	415	.35	145
Wing	218	1.00	218
Nacelles	100	.35	35
Fin	66	1.00	66
Tail	82	1.00	82
			546 sq.ft.

Hovering Download Area Estimate **

Fuselage	245	.35	86
Wing	148	1.00	148
Nacelles	100	.35	35
			269 sq.ft.

* In vertical rate of climb calculations, the total planform area is used to obtain the parasite drag load. For calculations of rates of climb at forward speeds, it is necessary to obtain the effect of parasite drag on the rotor in a vertical direction. Therefore, the induced area of the wing is subtracted from the total planform area and considered separately. The parasite drag area resulting is 546 sq.ft. minus 332 sq.ft. which equals 214 sq.ft.

** To get the hovering power required considering the effect of rotor downwash, an estimate is made of the area in the path of the downwash velocity.

6.2 Fixed wing characteristics - The Model 78 fixed wing of NACA 23012 to 23018 airfoil section has a 6.1 aspect ratio. The airfoil section characteristics for infinite aspect ratio obtained from reference [illegible] are corrected to the finite aspect ratio of 6.1 by equations:

$$\alpha_{AR} = \alpha_{\infty} + \frac{18.24\, C_{L_W}}{AR}$$

$$C_{D_{AR}} = C_{D_0} + \frac{C_{L_W}^2}{\pi \cdot AR}$$

A further correction on the lift-drag ratio is made to account for wing taper in accordance with reference 6.7. Figure 14 presents the corrected airfoil characteristics used in the aerodynamic performance estimates. The variation of lift coefficient with forward velocity in level flight is shown in figure 16.

6.3 Propeller characteristics -

6.3.1 Discussion - The preliminary turbo-prop installation consists of two, three-bladed full-feathering Aero Products propellers driven by two Allison Model 501 gas turbines through modified T-38 gear boxes. During helicopter operation, the propeller pitch is set at that which results in minimum power absorption by the propellers. For a preliminary estimate, this propeller setting is assumed to absorb [illegible] of the available engine shaft horsepower throughout the helicopter flight range. (See reference [illegible].) The preliminary propeller data are presented in section [illegible].

6.3.2 Propeller efficiencies - The preliminary propeller efficiency curve, figure 1[illegible], is estimated from the data presented in reference [illegible]. The method is as follows:

Step 1 - Assume velocity, altitude	220 knots, sea level
Step 2 - Determine engine power, propeller speed	2290 HP, 1760 rpm

Step 3 - Compute J

$$J = \frac{88\ V_{mph}}{nD} = \frac{88 \times 220 \times 1.15}{1760 \times 10} = 1.27$$

Step 4 - Compute C_p — $C_p = .210$

$$C_p = \frac{.5\,(SHP/1000)}{\rho/\rho_o\ (N/1000)^3 (D/10)^5}$$

$$C_p = \frac{.5 \times 2.29}{(1.76)^3\ (1)^5} = .210$$

Step 5 - Determine X and C_{P_X} — $X = .60$

Activity factor = 450 — $C_{P_X} = .350$

$$C_{P_X} = \frac{C_p}{X} = \frac{.210}{.60} = .350$$

Step 6 - Compute $J/(C_p)^{1/3}$

$$J/(C_p)^{1/3} = \frac{1.27}{(.210)^{1/3}} = \frac{1.27}{.605} = 2.10$$

Step 7 - From chart (reference 9.[illegible], page 150) read $\eta = .85$

Figure 19, propeller efficiency against velocity, is obtained by assuming various velocities and repeating the steps required to obtain propeller efficiency. These propeller efficiencies are used in transforming the shaft horsepower and net jet thrust to horsepower available for level flight performance calculations.

6.4 Flight limitations

6.4.1 Blade stall - Retreating blade stall is considered a limiting flight velocity criteria because of loss of control and objectionable vibration. NACA flight tests, reference 9.8, indicate that a retreating blade tip angle of attack of 12 degrees is the beginning of blade stall. Operation at tip angles greater than this causes increased profile power loss and objectionable vibration with loss of control occurring about 4 degrees above the initial stall angle.

Blade stall is primarily dependent upon the advance ratio and the aerodynamic blade loading (C_T/σ) which is a measure of the mean blade angle of attack. Figure 17 presents the relationship of initial stall C_T/σ with rotor shaft power parameter (P/L) for constant advance ratios, μ's. A discussion of this graph and its source is presented in section 6.5.4. For the Model 78, because of the aerodynamic blade loading and because of the effect of the fixed wing in forward flight, blade stall is avoided in the helicopter level flight condition, except for operation at or near C_{L_W} of fixed wing equal to zero. Other limits are more critical for the higher fixed-wing lift coefficients. In propeller flight, the increased drag losses, because of blade stall, are accounted for in the model test lift-drag ratio of the rotor; and since control is attained by a conventional aileron-elevator system, blade stall is not a limiting criteria.

6.4.2 Advancing blade velocity - An advancing blade velocity limitation is considered necessary to avoid increased power loss caused by Mach number drag divergence and objectionable vibration, fatigue, and control characteristics caused by blade lift loss and center of pressure movement. A limit of forward velocity plus rotational tip speed ($V + \Omega R$) of 900 feet per second is assumed,

which gives rise to a .80 Mach number at sea level. Reference 9.10 shows that rearward shifts of center of pressure are avoided if the Mach number is limited to this value. However, operation at higher advancing blade Mach numbers than .80 is probably practical because of the intermediate nature of the problem. Further wind tunnel research and full-scale flight test programs should provide additional information on this limitation.

6.4.3 Wing stall - The minimum propeller-driven flight speed is assumed to be dictated by the maximum wing lift coefficient. Actually, this is not a physical limit, since at these minimum speeds, the rotor is supporting a sufficient portion of the weight to maintain control. However, for analytical purposes, the maximum wing lift coefficient is used as a minimum velocity limit.

6.5 Pressure-jet flight condition

6.5.1 Hovering - The hovering aerodynamic efficiency of a jet rotor is best represented by the ratio of rotor thrust to jet thrust which may be written non-dimensionally as -

$$\frac{T}{F} = \frac{TR}{Q} = \frac{C_T \, \rho \pi R^2 (\Omega R)^2 R}{C_Q \, \rho \pi R^2 (\Omega R)^2 R} = \frac{C_T}{C_Q}$$

The hovering jet rotor torque requirements are the profile and the induced torques,

$$C_Q = C_{Q_o} + C_{Q_i}$$

For an ideally twisted rotor, the profile torque coefficient in terms of the NACA three-term drag polar which is representative of smooth, well-contoured

blades is by reference 8. ,

$$C_{Q_o} = \frac{\sigma}{8}\delta_o + 2/3\,\delta_1 \frac{C_T}{a^2} + \frac{4\delta_2}{a^2\sigma}\left[\frac{C_T}{a^2}\right]^2$$

and the induced torque coefficient is,

$$C_{Q_i} = \frac{.707(C_T)^{3/2}}{B}$$

For the Model 78, it is assumed that the profile drag, thus torque, is independent of blade twist and that the induced drag is increased ten percent to account for the variations from uniform inflow encountered with rectangular untwisted blades. The tip loss factor assumed is that presented by Sissingh in reference 8.13,

$$B = 1 - \frac{\sqrt{2C_T}}{b_R}$$

Since the jet thrust presented in reference 8.9 is gross internal thrust excluding jet external drag, the hovering rotor thrust - jet thrust ratio is modified to account for the drag torque of the jet units. An equivalent parasite area of .11 square feet per blade is assumed and the T/F ratio corrected accordingly,

$$\Delta C_Q = \frac{b_R f_J}{\rho\pi R^2} \cdot \frac{\rho(\Omega R)^2 R}{(\Omega R)^2 R} = \frac{b_R f_J}{2(\pi R^2)}$$

$$T/F = C_T/(C_{Q_o} + C_{Q_i} + \Delta C_Q)$$

Figure 15 presents the variation of the rotor thrust-jet thrust ratio with aerodynamic blade loading (C_T/σ). This figure is the basis of all hovering and vertical climb performance estimates.

6.5.2 Vertical climb - In a vertical climb, the rotor handles a greater mass of air (due to climb velocity) than in hovering and, therefore, needs to accelerate the air mass less to produce the same thrust. As a result, the induced power losses in a climb are less than those in hovering. Results of NACA tests (reference 9.12) were used to obtain the variation of the ratio of the excess horsepower to the effective climb horsepower with climb velocity (figure 16). The vertical rate of climb was calculated using this figure and the calculated excess horsepower.

$$V_v = HP_c \times \frac{33,000}{W}$$

The effective climb horsepower, HP_c, was determined with due consideration given the increased rotor lift required to overcome fuselage - fixed wing parasite drag in vertical climb. (See sample calculation).

6.5.3 Forward flight - Helicopter steady state forward flight performance is calculated by NACA methods of analysis (reference 9.8). Individual power losses are expressed as the energy dissipated per second by an equivalent drag force moving at the translational velocity of the aircraft. The sources of power loss are the rotor profile and induced drags, the jet unit external drag, the wing profile and induced drag, and the fuselage parasite drag.

An equivalent drag balance divided by lift is the basis of all steady state flight performance calculations. This drag balance is modified to account for a portion of the total lift being carried by the fixed wing with the resulting drag-lift equation reading:

$$D/L = L_R/L\left[(D/L_R)_o + (D/L_R)_i + (D/L_R)_J\right] + L_W/L\left[D/L_W\right]_W + \left[D/L\right]_P$$

In the helicopter flight condition, the jet external drag does not affect rotor characteristics such as blade angle and flapping coefficients, but does affect the power required, since gross internal thrust is used as jet thrust available. For these reasons, both $(D/L)_{TOT}$ including and excluding $(D/L)_J$ are calculated. (See sample calculation.) The power required is then calculated from the $(D/L)_{TOT}$ including the jet drag-lift ratio by:

$$HP_{(REQ)} = \left[D/L\right]_{TOTAL} \times \frac{L \times V}{550}$$

The drag-lift ratios used in the total drag-lift balance are developed individually:

<u>Rotor profile drag-lift ratio $(D/L)_o$</u> - The rotor profile drag-lift ratios for the various flight conditions are determined from the NACA charts of reference 9.8. These charts are developed for assumptions of zero twist and a profile drag polar ($C_D = .0087 - .0216\alpha + .40\alpha^2$) which is representative of smooth, accurately-contoured blades.

<u>Rotor induced drag-lift ratio $(D/L)_i$</u> - The rotor induced drag-lift ratio is calculated by treating the rotor as a lifting wing of $4/\pi$ aspect ratio. Thus:

$$(D/L_R)_i = \frac{C_{D_i}}{C_{L_R}} = \frac{C_{L_R}^{\ 2}}{\pi \, AR \, C_{L_R}} = \frac{C_{L_R}}{4}$$

<u>Fuselage parasite drag-lift ratio $(D/L)_p$</u> - The fuselage drag-lift ratio is calculated from the estimated equivalent parasite area. (See table I). Thus:

$$(D/L)_p = \frac{f \, 1/2 \, \rho \, V^2}{W} = \frac{fq}{W}$$

Jet external drag-lift ratio $(D/L)_J$ - The jet external drag-lift ratio is determined from an estimated cold drag coefficient of .145 which is based upon experience gained under the Air Materiel Command H-20 ram jet rotor contract. The maximum cross-sectional area of each pressure jet unit is 109 square inches. Therefore, the equivalent parasite area per unit is .11 square feet. Having established the equivalent parasite area, the jet drag-lift ratio may be determined by:

$$(D/L_R)_J \times L_R V = 1/2\pi \int_0^{2\pi} b_R f_J \; \rho/2 \; (\Omega R + V_{SIN\psi})^3 \, d\psi$$

which integrates to:

$$(D/L_R)_J = \frac{b_R f_J}{C_{L_R} \pi R^2} \left[1/\mu^3 + 3/2\mu \right]$$

For quick estimation of the jet drag-lift ratio, non-dimensional plots of $(D/L_R)_J$ against the reciprocal of the rotor lift coefficient for a ratio of $b_R f_J/\pi R^2$ equal to unity are presented as figures 20 and 20a. The value read from these charts must be multiplied by the actual ratio of cold jet equivalent parasite area to rotor disc area which is .00010 for Model 78.

For rotor-powered flight, the jet unit drag has no effect on the rotor characteristics, such as blade angle, angle of attack and a_1 flapping, but as already stated, does affect the power required. Therefore, the $(D/L_R)_J$ ratio is subtracted from the total D/L ratio for the determination of rotor characteristics other than power required.

Wing drag-lift ratio $(D/L)_W$ - The wing drag-lift ratio is obtained from a plot of the wing airfoil characteristics (figure 19) for the flight condition assumed, i.e., at the given wing lift coefficient. The variation of wing lift

coefficient with level forward flight velocity is presented as figure 10.

[illegible].4 Maximum rate of climb - In determining the maximum rate of climb in rotor-powered flight, it is necessary to calculate the rate of climb for several forward velocities because of the limiting criteria. Two curves are obtained, one, considering power limitation, and a second curve, considering blade stall as a limiting factor. The intersection of these two curves determines the maximum rate of climb. (See figure 16). In considering blade stall as a limit, it is convenient to obtain a plot of C_T/σ at initial stall for corresponding values of P/L and μ. Figure 17 is such a plot and is obtained by converting the C_L/σ values at initial blade stall from the NACA charts of reference 13 to C_T/σ for various μ and P/L values. This plot is used in conjunction with the assumed stall limit rotor load for checking the maximum rate of climb as shown in sample calculation 8.1.3.

The method used in constructing the rate of climb curves is the typical NACA analysis for rotor-powered flight.

$$P/L = (P/L)_o + (P/L)_i + (P/L)_J + (P/L) + (P/L)_w + (P/L)_c$$

A trial and error method is required to determine the actual operating conditions and power loss during climb. (See sample calculations 8.1.5.1 and 8.1.[illegible].)

[illegible].6 Turbo-prop flight condition

6.[illegible].1 Basis of analysis - In the turbo-propeller flight condition, the total weight of the aircraft is supported by a fixed-wing lifting surface combined

with an autorotating rotor. Wind tunnel model test programs contracted to the Office of Naval Research show that lightly loaded autorotating rotors may advance at far higher advance ratios than heretofore considered practical. Through these programs, rotor lift, drag, blade motion, blade stresses, fixed-wing interference, aircraft stability, and many other details have been analyzed and tested through a wide range of variables. The results of these model test programs and studies form the basis for the Model 78 aerodynamic performance estimates in the turbo-prop flight condition. Applicable test data are presented in figures 5, 6, 7, and 8; for further data, see MAC Engineering Letters, reference 9.18.

Figure 5, "Rotor Lift Coefficient Against Advance Ratio", presents a comparison of McDonnell wind tunnel tests at the high advance ratios and other pertinent test data from previous NACA programs. Figure 6 gives a mean curve used in the performance estimates.

Figure 7, "Rotor Lift-Drag Ratio Against Advance Ratio", shows comparative results of NACA tests with a ten-foot rotor model (reference 9.17) and with a full-scale Pitcairn rotor (reference 9.16) and McDonnell tests with an eight-foot rotor model, together with the results of McDonnell theory. Accounting for Reynolds number effect, all the different test results and theoretical results are in satisfactory agreement. Figure 8 gives the rotor lift-drag curve used in the Model 78 preliminary performance estimates.

6.6.2 Forward flight - Level flight power required for forward velocities is obtained in a manner similar to that described in the section on rotor-powered forward flight (section 6.5.3). A modified drag-lift equation is used for turbo-prop flight. The power loss due to drag of the rotor is based on autorotational

wind tunnel data which does not separate the profile and induced losses in the rotor (see figure 8). In these tests, which compare favorably with other wind tunnel and theoretical data, the rotor and its hub are considered as one unit. Therefore, it is only necessary to add the tip jet drag contribution to the rotor for a drag power loss due to the autorotating rotor.

It should also be noted that the parasite drag area used for the parasite drag loss differs in the rotor-powered and turbo-prop power required calculations. This difference is due to the fact that the hub drag is included with that measured for the rotor in the autorotational test data. In the rotor-powered flight, the hub drag is taken as a component of the parasite drag area for the whole ship and included with the parasite drag power loss.

The resulting drag-lift equation is as follows:

$$D/L = L_R/L \left[(D/L_R)_R + (D/L_R)_J \right] + L_W/L \left[D/L_W \right]_W + \left[D/L \right]_P$$

The power required is then calculated from the D/L_{TOTAL} using the following equation:

$$HP_{(REQ)} = (D/L)_{TOTAL} \times \frac{L \times V}{550}$$

(See sample calculation 9.1.4).

The percent load carried by the rotor throughout the flight velocity range is presented as figure 11. The dash lines represent the percent load carried by the rotor in helicopter flight, while the solid lines are for turbo-prop flight at various autorotating rotor tip speeds.

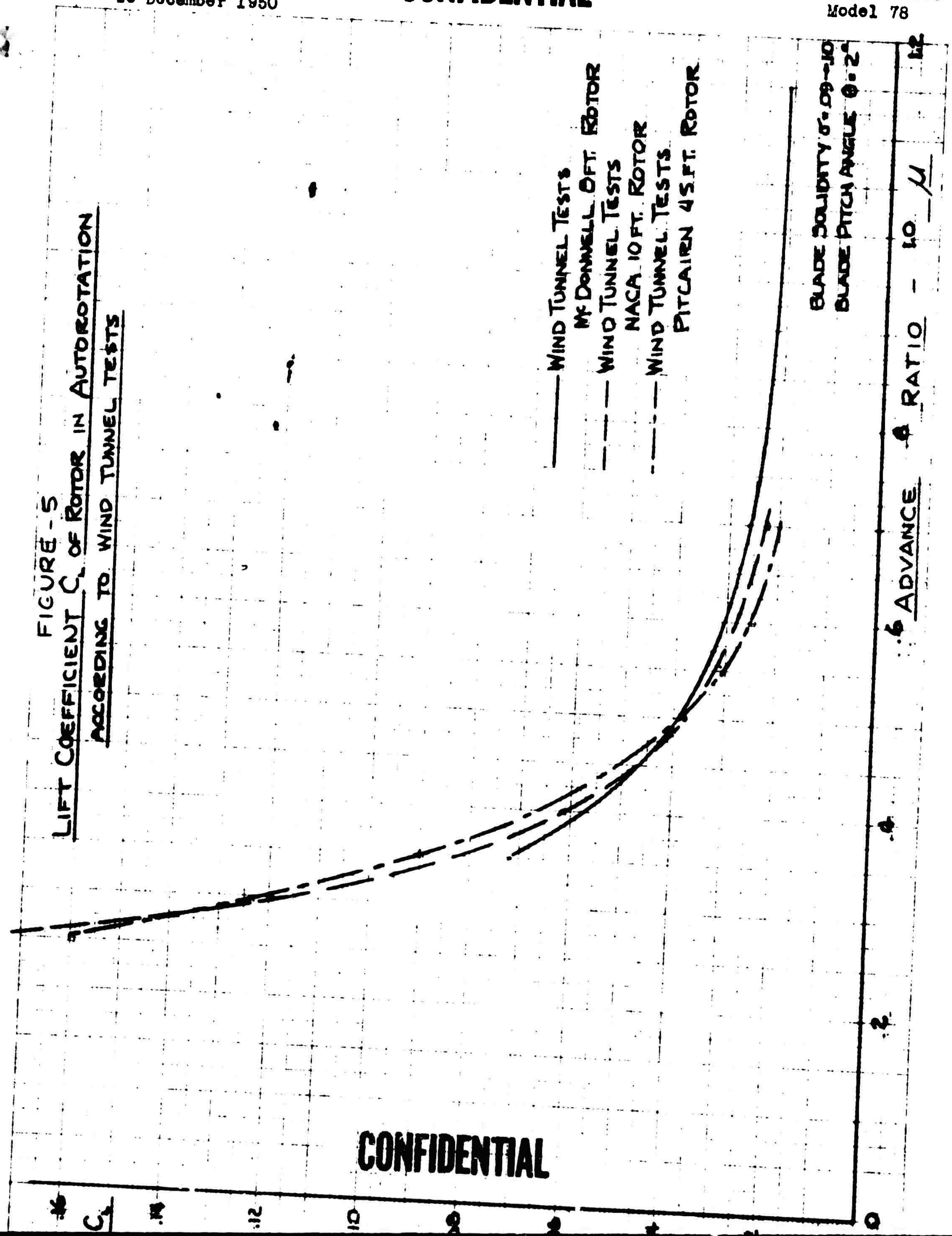
FIGURE - 5
LIFT COEFFICIENT C_L OF ROTOR IN AUTOROTATION
ACCORDING TO WIND TUNNEL TESTS
WIND TUNNEL TESTS McDONNELL 8FT. ROTOR
WIND TUNNEL TESTS NACA 10FT. ROTOR
WIND TUNNEL TESTS PITCAIRN 45FT. ROTOR
BLADE SOLIDITY σ = .09 - .10
BLADE PITCH ANGLE θ = 2°
ADVANCE RATIO - μ
0
.2
.4
.6
.8
1.0
1.2
C_L
.12
.10

CONFIDENTIAL

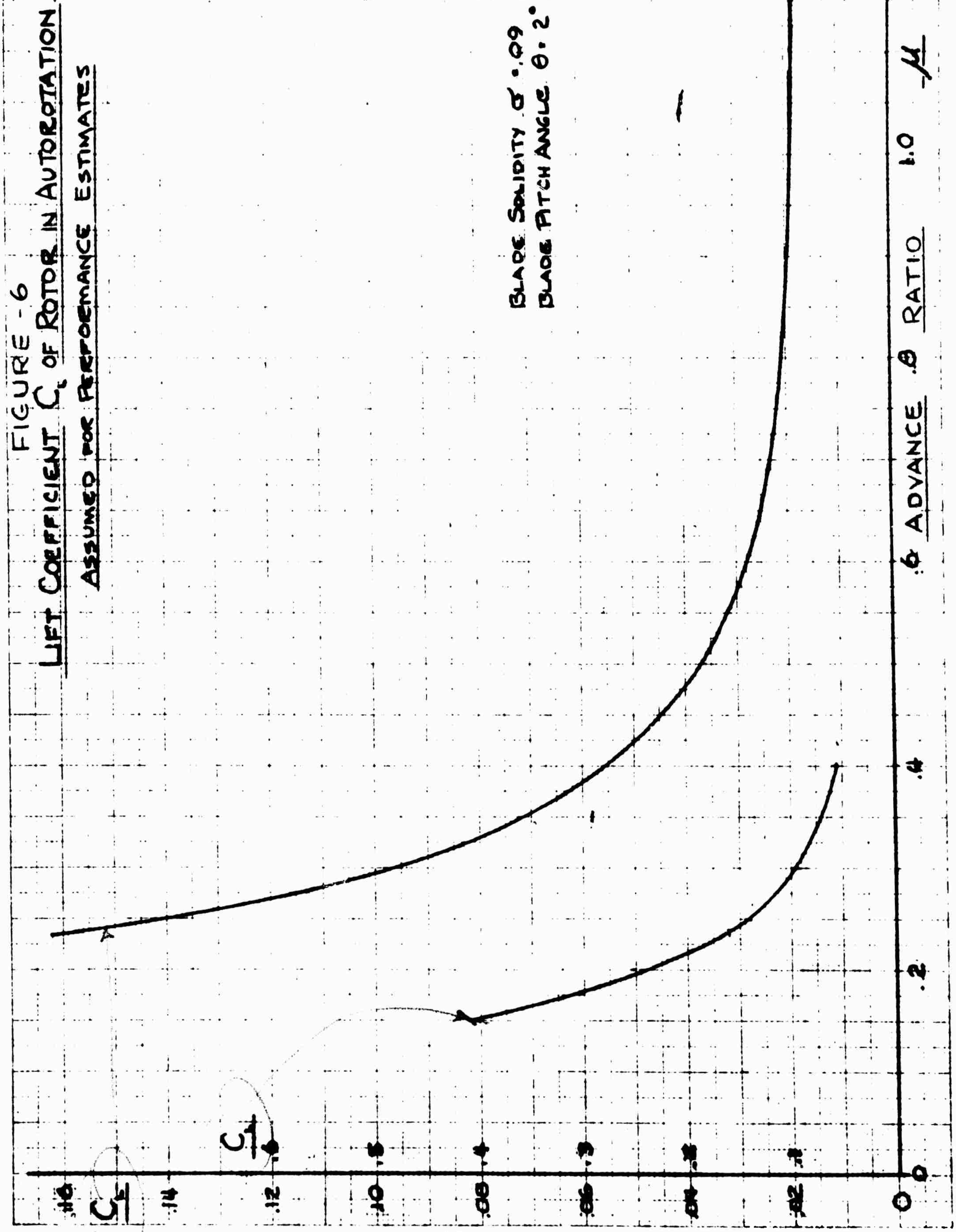

CONFIDENTIAL

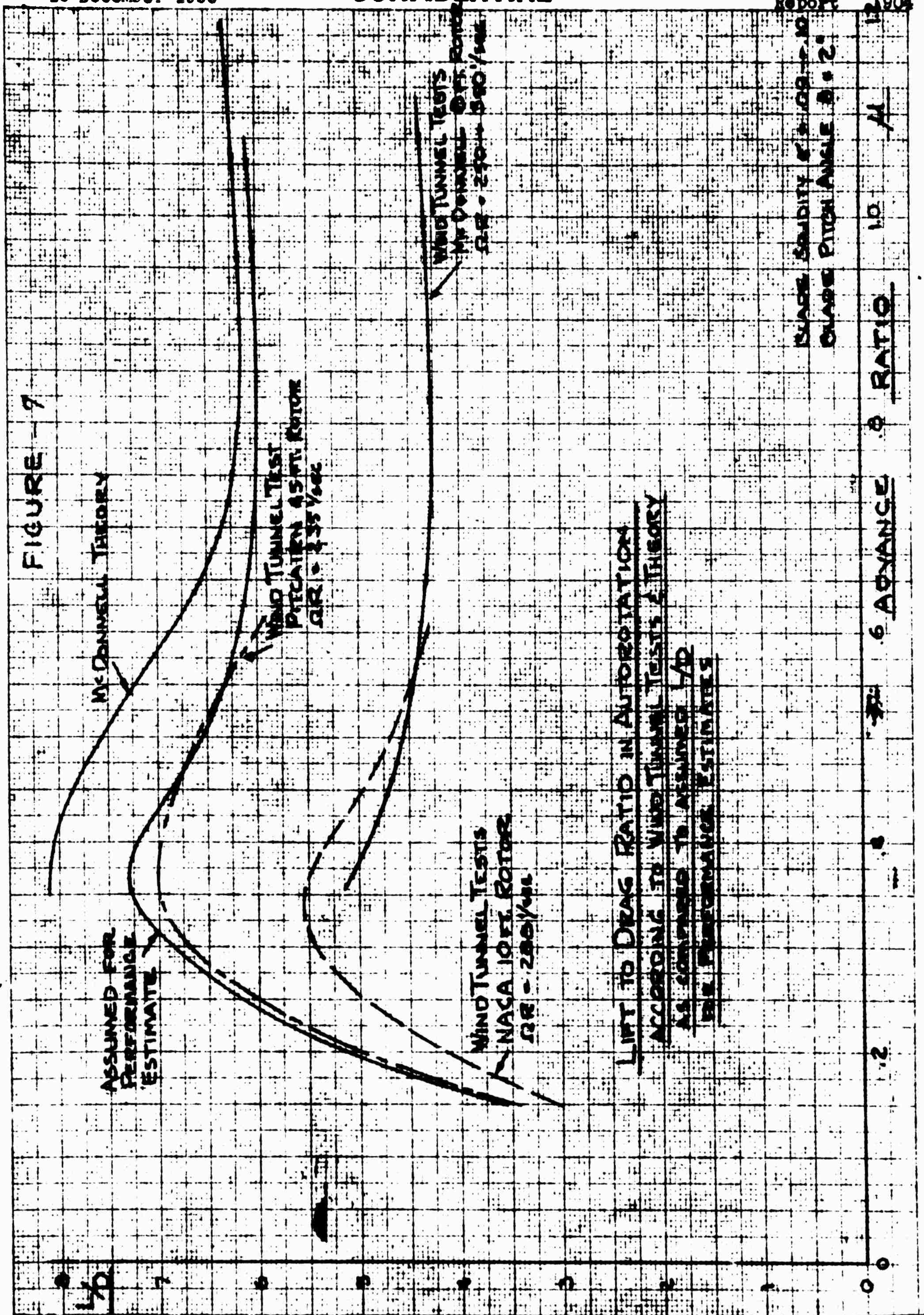
FIGURE - 7
McDONNELL THEORY
WIND TUNNEL TEST PITCAIRN 45 FT. ROTOR ΩR = 235'/SEC
WIND TUNNEL TESTS McDONNELL 10 FT. ROTOR ΩR = 270 - 350'/SEC
ASSUMED FOR PERFORMANCE ESTIMATE
WIND TUNNEL TESTS NACA 10 FT. ROTOR ΩR - 280'/SEC
LIFT TO DRAG RATIO IN AUTOROTATION ACCORDING TO WIND TUNNEL TESTS & THEORY AS COMPARED TO ASSUMED L/D FOR PERFORMANCE ESTIMATES
BLADE SOLIDITY σ = .08 - .10
BLADE PITCH ANGLE θ = 2°
ADVANCE RATIO μ
L/D
0
.2
.6
.8
1.0
1.2

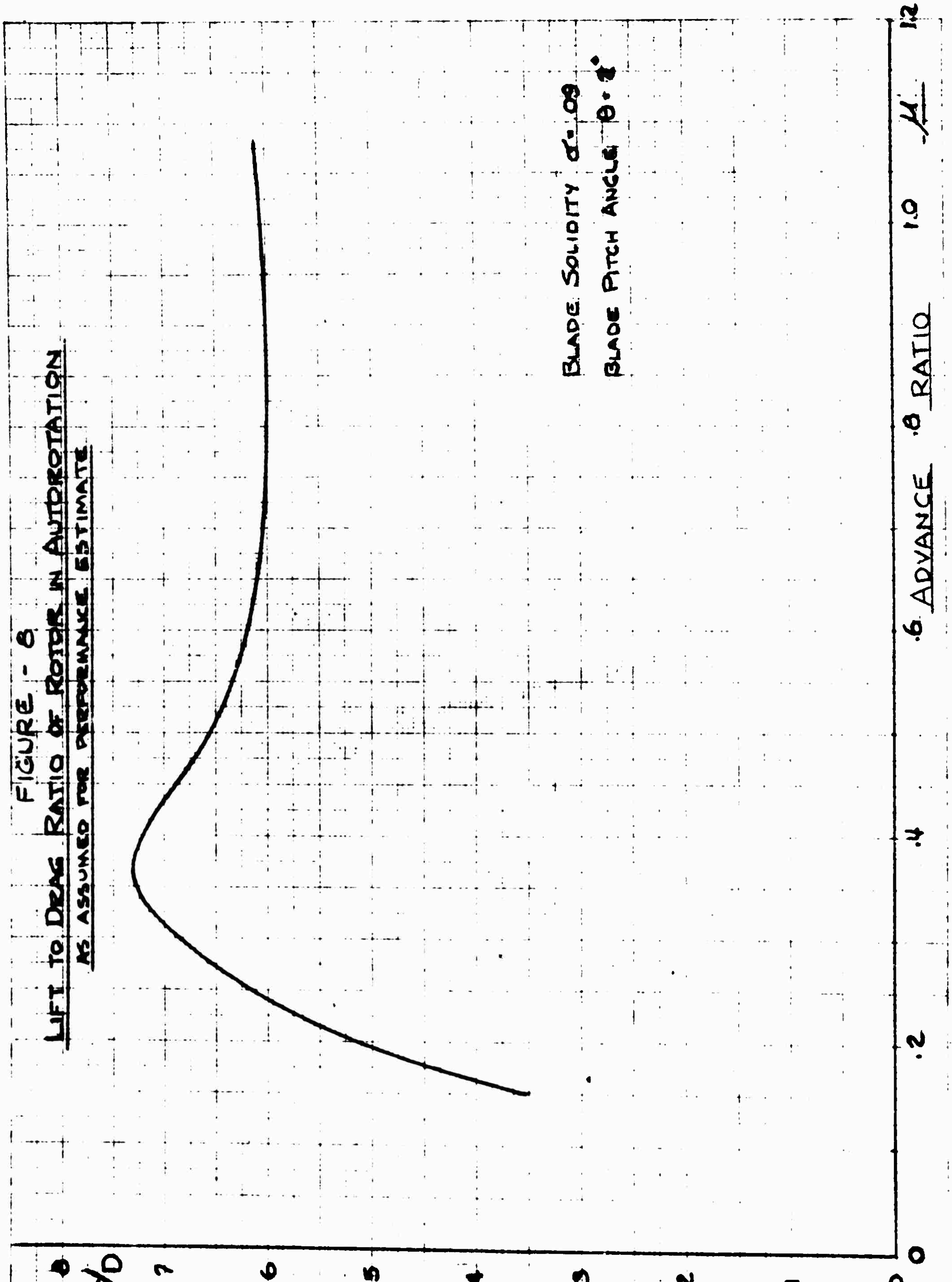
FIGURE - 8
LIFT TO DRAG RATIO OF ROTOR IN AUTOROTATION
AS ASSUMED FOR PERFORMANCE ESTIMATE
BLADE SOLIDITY σ = .09
BLADE PITCH ANGLE θ =
ADVANCE RATIO μ
L/D
0
.2
.4
.6
.8
1.0
1.2
0
1
2
3
4
5
6
7
8

[illegible].3 Maximum rate of climb - From the "horsepower required" curve, figure [illegible], the point of maximum excess [illegible] [illegible] the [illegible] for the maximum rate of climb. The excess horsepower at this velocity is [illegible] available for climb and applied in [illegible] [illegible]:

Max. [illegible] = [illegible] [illegible] [illegible],000 = ft./min.

6.7 Autorotation characteristics - The [illegible] [illegible]-[illegible] [illegible] [illegible] [illegible] wing gives this configuration [illegible] over the conventional [illegible] [illegible] autorotation. [illegible] benefit of [illegible] [illegible] is [illegible] [illegible] in [illegible] descent [illegible] the [illegible] operation [illegible] [illegible]. [illegible] lotted [illegible] [illegible], the [illegible] descent are calculated from the [illegible]:

[illegible] = [illegible]

The [illegible] values for this equation [illegible] from the level flight [illegible] required calculations for turbo-prop operation. [illegible], the rotor is autorotating. Taking these drag-lift ratios [illegible] for total power-off flight at their respective forward flight velocities, [illegible] descent are calculated [illegible] the above equation.

V. [illegible] AVAILABLE

[illegible] [illegible] - [illegible] detailed explanation of [illegible] power plant [illegible] and [illegible] to obtain power available for [illegible] flight [illegible] are con- [illegible] in r[illegible] . . .

[illegible] will [illegible] that [illegible] available curves for tip [illegible] are [illegible] per [illegible]. [illegible] found [illegible] to [illegible] the tip speed in hovering, vertical fli[illegible], [illegible] over [illegible] in order to obtain stall-free operation and [illegible] control characteristics. For the preliminary performance estimat[illegible], it is [illegible] that this small [illegible] in tip speed would effect no appreciable [illegible] in [illegible] the available tip jet thrust or the [illegible] specific [illegible] consumption. The data taken from refer- ence [illegible] may be used directly as far as losses are concerned, since the inlet duct losses and losses for propeller operation at low pitch [illegible] -jet flight are accounted for in the [illegible] of [illegible] reference [illegible].

[illegible]

8.1 Sample calculation

8.1.1 [illegible] of ground effect

Altitude	=	Sea level
Gross weight	=	30,000 pounds
Disc area	=	3320 sq. ft.
Rotor tip speed	=	7[illegible]0 ft./second
Rotor solidity	=	.09
Rotor disc loading	=	$\frac{30{,}000 + \text{downwash load on fuselage}}{3320}$

Assuming hovering downwash load to be 1190 pounds, compute the induced velocity,
see below

$$v_i = \sqrt{\frac{T}{2\rho A}} = \sqrt{\frac{30{,}000 + 1190}{2\rho\,(3320)}} = 44.5 \text{ ft./second}$$

Allowing increase of 36% for inflow contraction,

$$(44.5)\,1.36 = 60.5 \text{ ft./second}$$

[illegible] area, f = 2[illegible]9 sq.ft. (See page [illegible].)

Downwash load:

$$D = \tfrac{1}{2}\rho v_i^2 f = \rho/2\,(60.5)^2\,2[illegible]9 = 1190 \text{ pounds}$$

$$C_T = \frac{T}{\rho A(\Omega R)^2} = \frac{30{,}000 + 1190}{\rho\,(3320)(7[illegible]0)^2} = .00704$$

$$C_T/\sigma = \frac{.00704}{.09} = .0782$$

From figure [illegible], hovering T/F = 11.[illegible]

required jet thrust = $\frac{31180}{11.[illegible]}$ = [illegible] pounds

required hovering horsepower = $\frac{[illegible]}{550}$ = [illegible] HP

[illegible].1.2 Hovering power required (considering [illegible]) [illegible] Day - sea level

ρ = .002242

C_T = $\frac{31180}{[illegible](.00[illegible])([illegible])^2}$ = .00[illegible]

C_T/σ = $\frac{.00748}{.09}$ = .08[illegible]

T/F = 10.34 (figure 1[illegible])

$\frac{31180}{10.34}$ = 2[illegible] pounds jet thrust

required rotor HP = $\frac{2[illegible] \times [illegible]}{550}$ = 3[illegible]20 HP

From figure 30, reference [illegible], the tip jet thrust available [illegible] day is 4420 pounds at Ω = 700 ft./sec. Assuming equal available thrust at Ω = [illegible] ft./sec., the horsepower available becomes

$\frac{4420 \times 7[illegible]0}{[illegible]50}$ = [illegible]

$\frac{[illegible] \times [illegible]}{[illegible]}$ = [illegible]

[illegible] requirement [illegible] reference [illegible]. [illegible] that hovering [illegible] power should [illegible].

[illegible].1.[illegible] Vertical rate of climb

Gross weight	=	30,[illegible] pounds
Rotor diameter	=	[illegible]
Rotor tip speed		[illegible]
Rotor solidity		.[illegible]
Parasite area (planform)	=	[illegible] ft.^{2} (see page 20)
Hovering download	-	11[illegible] pounds

From hovering power required [illegible] -

$$HP(req) = [illegible]$$

$$HP(avail) = [illegible]$$

$$HP(climb) = HP(avail) - HP(req)$$

$$HP(climb) = [illegible] - 5[illegible]65 = 2[illegible]$$

$$\text{Approx. [illegible]} = \frac{[illegible] \times 33,000}{30,000} = [illegible] \text{ ft./min.}$$

To allow for losses [illegible], assume vertical [illegible] equals [illegible]000/min. ([illegible] = 1.[illegible] from figure 1)

[illegible]:

[illegible] = 1 2 [illegible].

[illegible]:

[illegible]

[illegible]:

1. [illegible]

[illegible] = [illegible] / 50,[illegible]

8.1.4 Pressure-jet level flight power required

Altitude = Sea level

Gross weight = 30,000 lbs.
Rotor disc area = 3320 ft.^{2}
Rotor tip speed = 700 ft./sec.
Rotor solidity = .09

Total parasite area = 18.32 ft.^{2}
Fixed wing area = 332 ft.^{2}
Wing lift coefficient = .5
L/D for wing = 20.9

μ	ASSUMED	.10	.15	.20	.25	.30	.35
V	FT./SEC.	70	105	140	175	210	245
V_{KN}	KNOTS	41.5	62.3	83	103.6	124.5	145.2
q	$\frac{1}{2}\rho V^2$	5.82	13.12	23.3	36.4	52.4	71.4
L_W	$C_{L_W} \times A_W \times q$	965	2180	3865	6040	8700	11850
L_R	$L - L_W$	29035	27820	26135	23960	21300	18150
C_{L_R}	$L_R/3320\,q$	1.50	.639	.348	.1983	.1224	.0767
$1/C_{L_R}$		.67	1.57	2.88	5.05	8.18	13.05
C_{L_R}/σ		[illegible]	7.10	3.87	2.21	1.36	.85
$(D/L_R)_o$	NACA CHARTS	.1750	.1170	.0930	.0840	.0845	.0910
$(D/L_R)_i$	$C_{L_R}/4$	.3750	.1600	.0846	.0496	.0306	.0192
$(D/L_R)_J$	FIGURE 20 & 20a	.0680	.0475	.0330	.0350	.0340	.0360
$(D/L_R)_R$	$\frac{L_R}{L}\left[(\frac{D}{L})_o + (\frac{D}{L})_i + (\frac{D}{L})_J\right]$	.5980	.3010	.1872	.1345	.1066	.0865
$(D/L)_P$	$18.32\,q/L$	.0036	.0020	.0142	.0222	.0320	.0435
$(D/L)_W$	$\frac{L_W}{L}\left[1/(\frac{L}{D})_W\right]$	.0015	.0035	.0062	.0097	.0139	.0190
$(D/L)_{TOT}$	$(\frac{D}{L})_R + (\frac{D}{L})_P + (\frac{D}{L})_W$	.6031	.3125	.2076	.1604	.1525	.1510
F_J	$(\frac{D}{L})_{TOT} \times \frac{L \times V}{700}$	1808	1410	1245	1249	1373	1535
HP(REQ.)	$F_J \times \frac{700}{550}$	2300	1795	1585	1590	1748	2020
D/L_R	*	.5552	.2894	.2010	.1735	.1797	.2137
θ	NACA CHARTS	9.0°	8.0°	7.0°	7.45°	7.55°	8.6°

* D/L_R calculated as the sum of the induced, profile, wing and fuselage drag-lift ratios based upon rotor lift in order to determine $[D/L_R]_o$ and blade angle θ (See section 8.5.3).

8.1.5 Turbo-prop level flight power required
[illegible] level $\rho = .002378$

Gross weight = [illegible] lbs. Parasite drag area = 14.[illegible] ft.^{2}
Fixed-wing area = [illegible] ft.^{2} Rotor tip speed = 7[illegible] ft./sec.
Rotor disc area = [illegible] ft.^{2} Rotor solidity = .0[illegible]

μ	Assumed	.1[illegible]	.20	.2[illegible]	.30	.3[illegible]
C_{L_R}	Figure 6	.[illegible]1	.24	.142	.[illegible]	.[illegible]
$1/C_{L_R}$		2.44	4.1[illegible]	7.0[illegible]	10.42	14.[illegible]
V	ft./sec.	10[illegible]	1[illegible]0	17[illegible]	210	24[illegible]
V_{KN}	knots	[illegible].2	[illegible]	10[illegible]	12[illegible]	1[illegible].?
q	$\frac{1}{2}\rho V^2$	13.1	[illegible].23	[illegible].4	[illegible]	71.5
L_R	C_{L_R} ([illegible])q	17840	18[illegible]50	171[illegible]0	16700	1[illegible]850
L_W	$L - L_R$	12160	114[illegible]0	128[illegible]0	13300	1[illegible]150
C_{L_W}	$L_W/332q$	2.795	1.4[illegible]	1.0[illegible]4	.7[illegible]	.[illegible]
$(L/D_W)_W$	Figure 18	[illegible]	10.[illegible]	1[illegible].0	17.[illegible]	20.[illegible]
$(L/D_R)_R$	Figure 8	[illegible]	[illegible].15	[illegible].15	6.35	[illegible]
$(D/L_R)_R$	*		.1200	.[illegible]	.0[illegible]1[illegible]	.[illegible]7[illegible]
$(D/L_T)_J$	**		.0[illegible]	.0232	.[illegible]	.021[illegible]
D/L_P	$14q/L$		.01[illegible]	.[illegible]170	.02[illegible]	.0[illegible]3
$(D/L_W)_W$	$L_W/L\left[1/(L/D)_W\right]$		.0[illegible]	.0[illegible]06	.0253	.[illegible]216
D/L_{tot}	$D/L_R+D/L_J+D/L_P+D/L_W$		.198[illegible]	.1[illegible]1	.1[illegible]	.1[illegible]
HP(req)	$D/L_{tot}\times(L \times V)/550$		1519	1[illegible]15	17[illegible]0	20[illegible]

* $(D/L_R)_R = L_R/L\left[1/(L/D_R)_R\right]$

** $(D/L_T)_J = L_R/L$ [Value from Figure 20, [illegible] [illegible] .00[illegible]10]

[illegible].1.[illegible] Gross [illegible]

Gross weight = [illegible], [illegible] l[illegible].

Disc area = [illegible] [illegible].

Rotor solidity = .[illegible]

[illegible].1.[illegible].1 Considering blade stall at the [illegible] [illegible]r:

Assume μ = .1[illegible], hence velocity = 1[illegible] ft./sec at Ω[illegible] = 700 ft./sec.

Assume [illegible] R/C = 12[illegible]0 ft./min.

Glide angle is:

$$\tan \angle = \frac{21}{105}$$

Angle = 11.3°

Wing angle of attack = -11.[illegible] + [illegible].[illegible] = -[illegible].[illegible]°

From figure 1[illegible], C_{L_w} = -.[illegible]2   L/D = 1[illegible].[illegible]

Wing load = $C_{L_w} \times \rho/2 \times A_w \times V^2$

= -.[illegible] × .[illegible] [illegible] 2 × [illegible] [illegible]

= -2[illegible] lbs.

Fuselage drag load = A × q

= 214 × $\rho/2$ $(21)^2$ = 112 lbs.

Total load on rotor = 30,[illegible] + 23[illegible]0 + 112 = 3[illegible],[illegible]2 lbs.

Assuming 32,462 lbs. to be stall limit rotor load at 105 ft./sec., calculate power required for this climb condition:

$$C_T/\sigma = \frac{32,462}{\sigma \times \rho \times 5520(700)^2} = .0955$$

Figure 17 shows for initial stall C_T/σ of .0955 at μ = .15, that P/L for rotor = .54

For P/L = .54, calculate the following using NACA charts:

$$C_L/\sigma = \frac{32,462}{\sigma \times \rho/2 \times 5520(105)^2} = 8.31 \quad ; C_L = .749$$

From NACA charts and by the methods of section 6.[illegible].3

$$(D/L)_o = .1180$$

$$(D/L)_i = .1870$$

$$(D/L)_J = .0400$$

$$(D/L)_p = .0074$$

$$L_w/L(D/L)_w = \underline{.0037}$$

$$.3561 = (D/L)_{TOTAL}$$

$$(D/L)_c = .5400 - .3561 = .1839$$

$$HP_{CLIMB} = .1839 \times \frac{32462 \times 105}{550} = 1140$$

$$R/C = 1140 \times \frac{33000}{30000} = \underline{1250 \text{ ft./min.}}$$

which checks the assumed value of 1200 ft./min.

[illegible].1.[illegible].2 Considering power available as the limiting factor:

Assume $\mu = .15$, hence velocity = 105 ft./sec. at ΩR = 700 ft./sec.

Rotor max R/C = 3640 ft./min.

Climb angle:

$$\tan \angle = \frac{60.6}{105}$$

$$\text{Angle} = 30°$$

Wing angle of attack = $-30 + 3 = -27°$

From figure 18, $C_{L_W} = -1.38$ $\qquad$ $L/D = 8.7$

Wing download = $-1.38 \times \rho/2 \times 332 \times 11,700$

$= -9750$ lbs.

Parasite drag load = $A \times q$

$= 214 \times \rho/2(60.6)^2 = 936$ lbs.

Total rotor load = $30,000 + 9750 + 936 = 40686$ lbs.

$$\text{Rotor } D/L = \frac{HP \times 550}{L \times V} = \frac{3600 \times 550}{40686 \times 105} = .348$$

$$\text{Rotor } C_L/\sigma = \frac{40,686}{\sigma \times \rho/2 \times 3320(105)^2} = 10.46$$

From NACA charts at D/L = .50, which is permissible, since $(D/L)_o$ varies but little with D/L change in the low advance ratio range. (See reference 9.8).

$$(D/L)_o = .1205$$

$$(D/L)_i = .2355$$

$$(D/L)_J = .0320$$

$$(D/L)_P = .0059$$

$$L_W/L(D/L)_W = \underline{.0275}$$

$$.4214 = (D/L)_{TOTAL}$$

$$(L/D)_c = .8480 - .4214 = .4266$$

$$HP_{CLIMB} = .4266 \times \frac{40686 \times 105}{550} = 3320$$

$$R/C = 3320 \times \frac{33000}{30000} = \underline{\underline{3650 \text{ ft./min.}}}$$

which checks the assumed value of 3640 ft./min.

8.1.7 Propeller propulsion maximum rate of climb

Excess horsepower at 140 knots = 1680

(Reference figure 9.)

Therefore, $R/C = \frac{1680 \times 33000}{30000} = \underline{1850 \text{ ft./min.}}$

8.1.3 Normal fuel load calculation

The calculated total fuel load requirements of the Model 78 consist of the following:

a. 15 minutes at normal rated power

(1) 2 minutes hovering

(2) 13 minutes at 100-knot cruising

b. 100-mile combat radius at cruise speed of 220 knots

c. 10% reserve

d. 5% increase in all SFC for service variation

Hovering fuel required = 6770 lbs./hr. (Conservative estimate from reference 9.9)

Turbo-prop fuel required = 2876 lbs./hr. (reference [illegible])
(normal rated power)

Turbo-prop fuel required = 2610 lbs./hr. (reference 9.9)
(at cruise horsepower)

15 minutes warm-up

$$6770 \times 1.05 \times \frac{2}{60} = 237 \text{ lbs.}$$

$$2876 \times 1.05 \times \frac{13}{60} = 654 \text{ lbs.}$$

100-mile cruise radius at 220 knots

$$2610 \times 1.05 \times \frac{200}{220} = 2490 \text{ lbs.}$$

10% reserve = 376 lbs.

TOTAL = 3757 lbs.

FIGURE - 9

MODEL 78

LEVEL FLIGHT PERFORMANCE

POWER REQUIRED vs VELOCITY

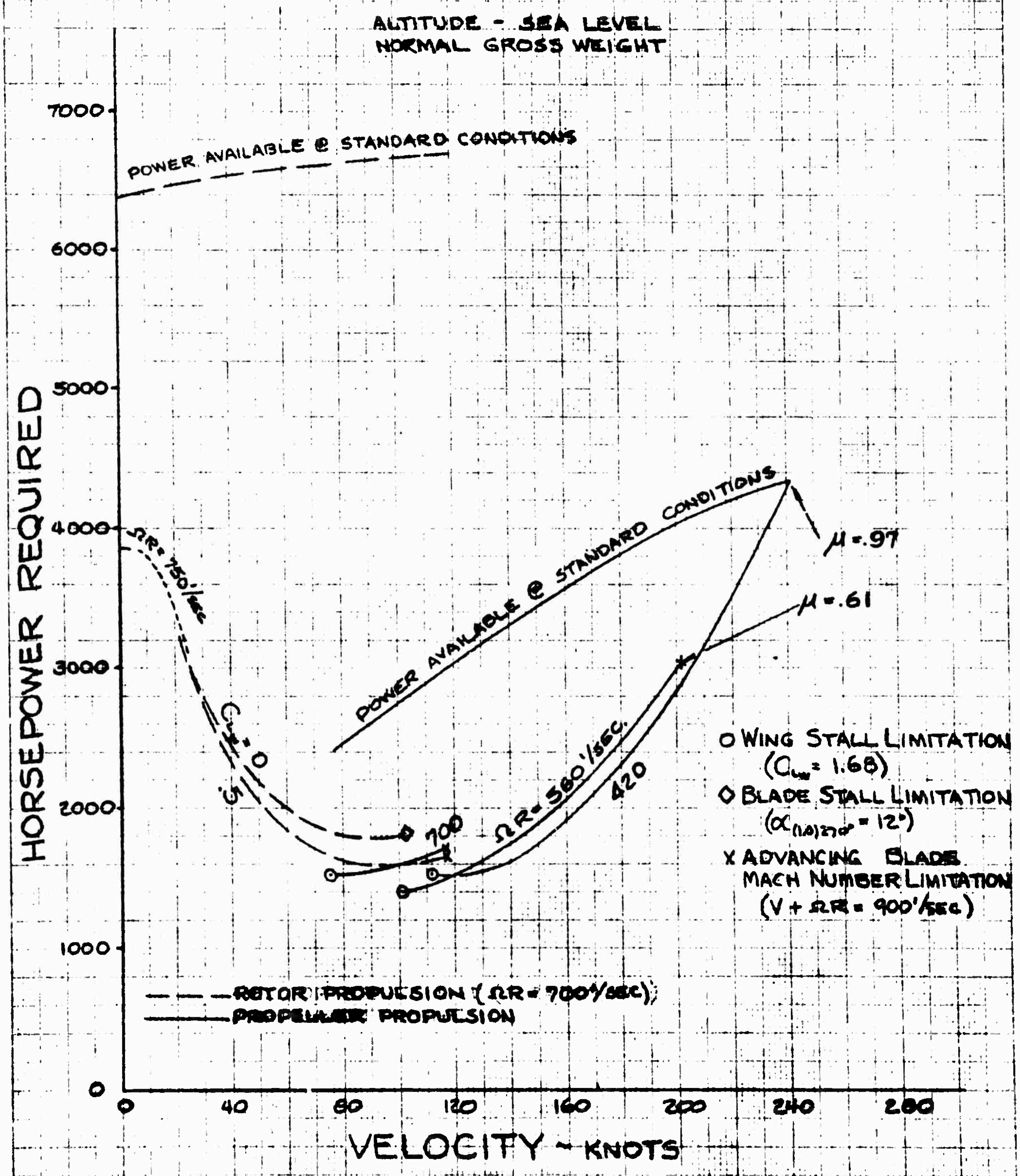

FIGURE [illegible]

MODEL 78

LEVEL FLIGHT PERFORMANCE

WING LIFT COEFFICENT VS VELOCITY

ALTITUDE - SEA LEVEL

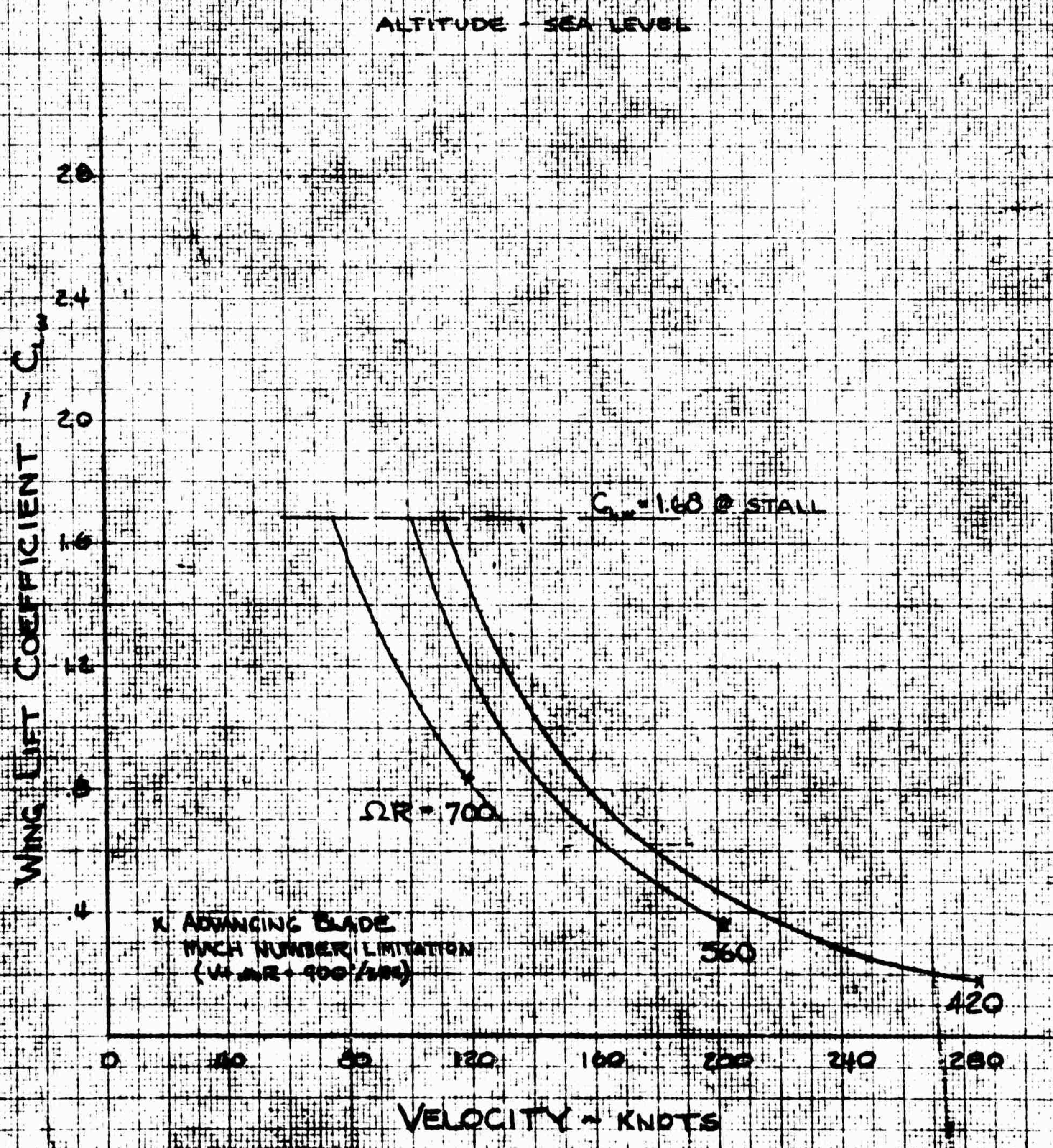

CONFIDENTIAL

20 December 1950

FIGURE - 12

MODEL 78

LEVEL FLIGHT PERFORMANCE

ROTOR LOAD vs VELOCITY

GROSS WT = 30,000 LBS.
ALTITUDE - SEA LEVEL

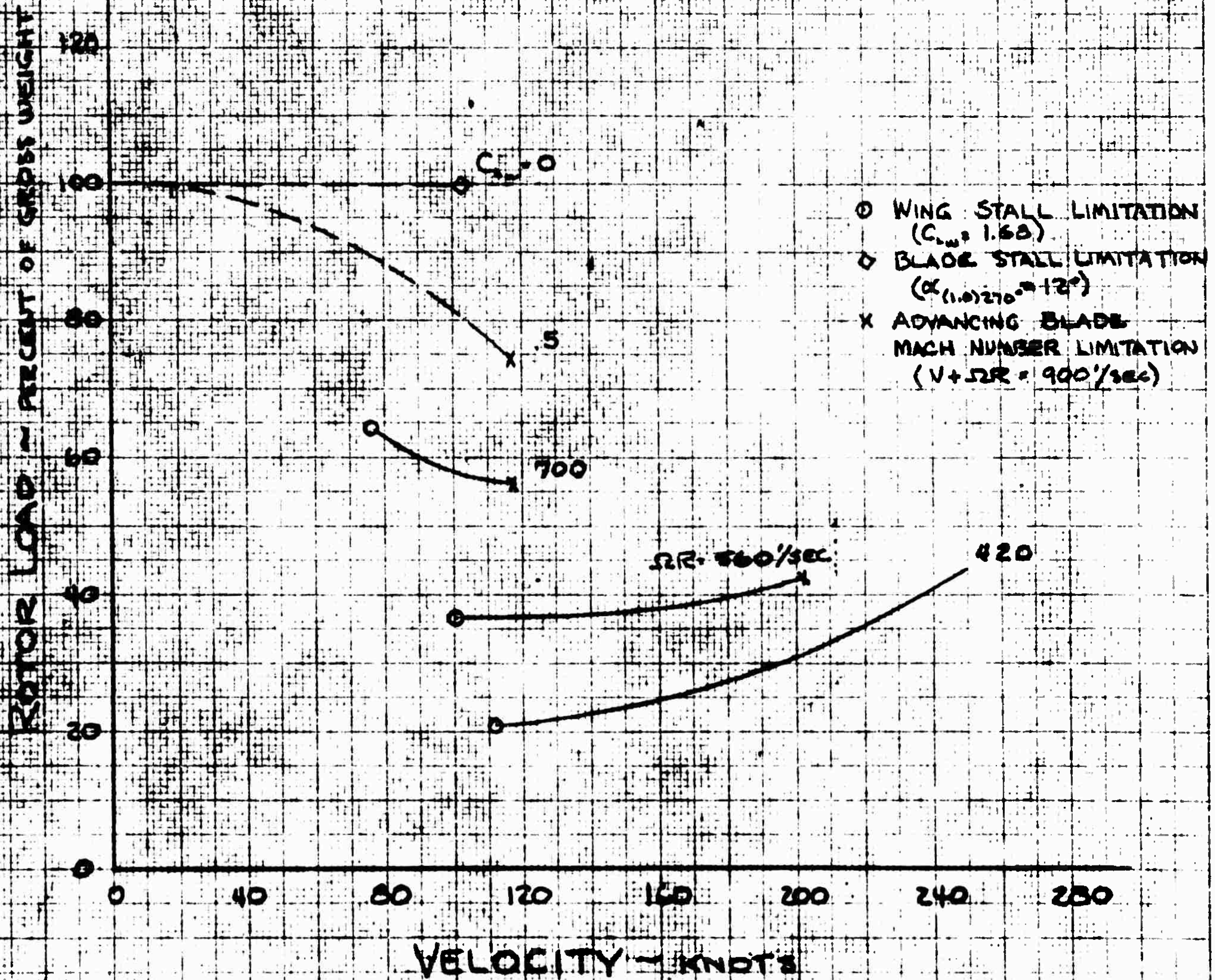

FIGURE - 12

MODEL 78

LEVEL FLIGHT PERFORMANCE

MAXIMUM VELOCITY vs ROTOR TIP SPEED

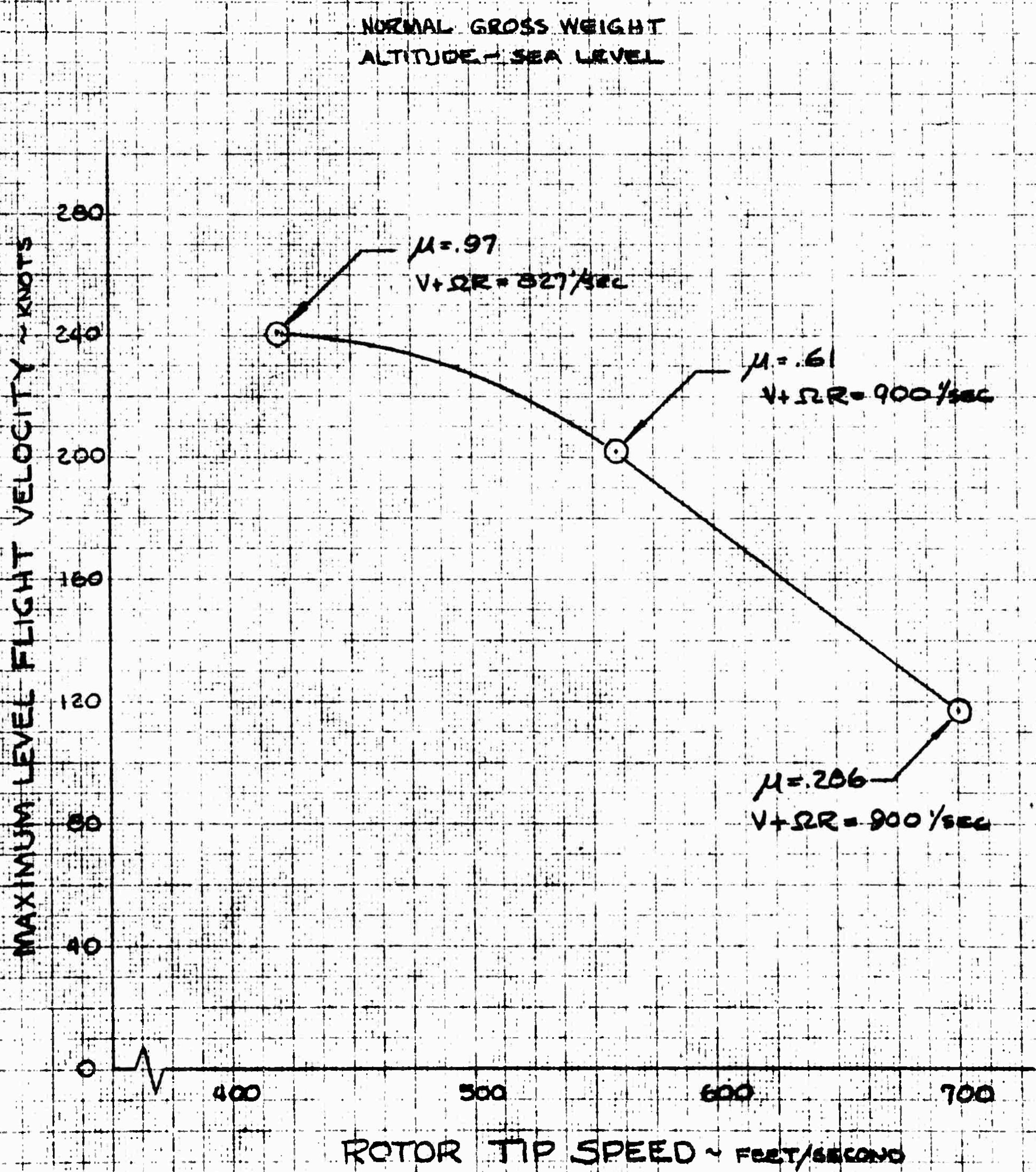

FIGURE - 13

MODEL 78

MAXIMUM RATE OF CLIMB vs VELOCITY

NORMAL GROSS WEIGHT
ALTITUDE - SEA LEVEL

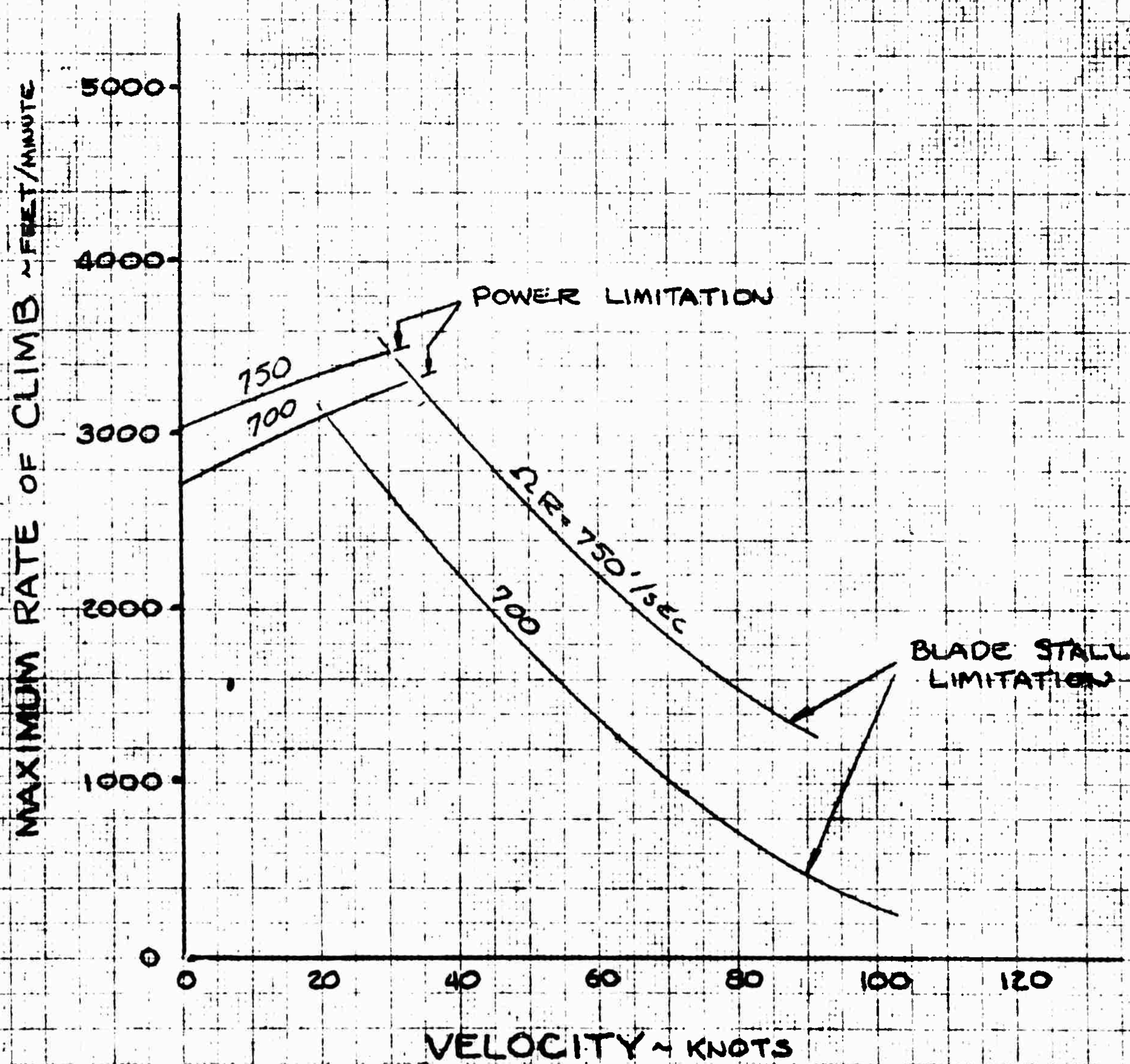

CONFIDENTIAL

20 December 1950

FIGURE - 18

MODEL 78

AUTOROTATIVE FLIGHT

MINIMUM RATE OF DESCENT vs VELOCITY

NORMAL GROSS WEIGHT
ALTITUDE - SEA LEVEL

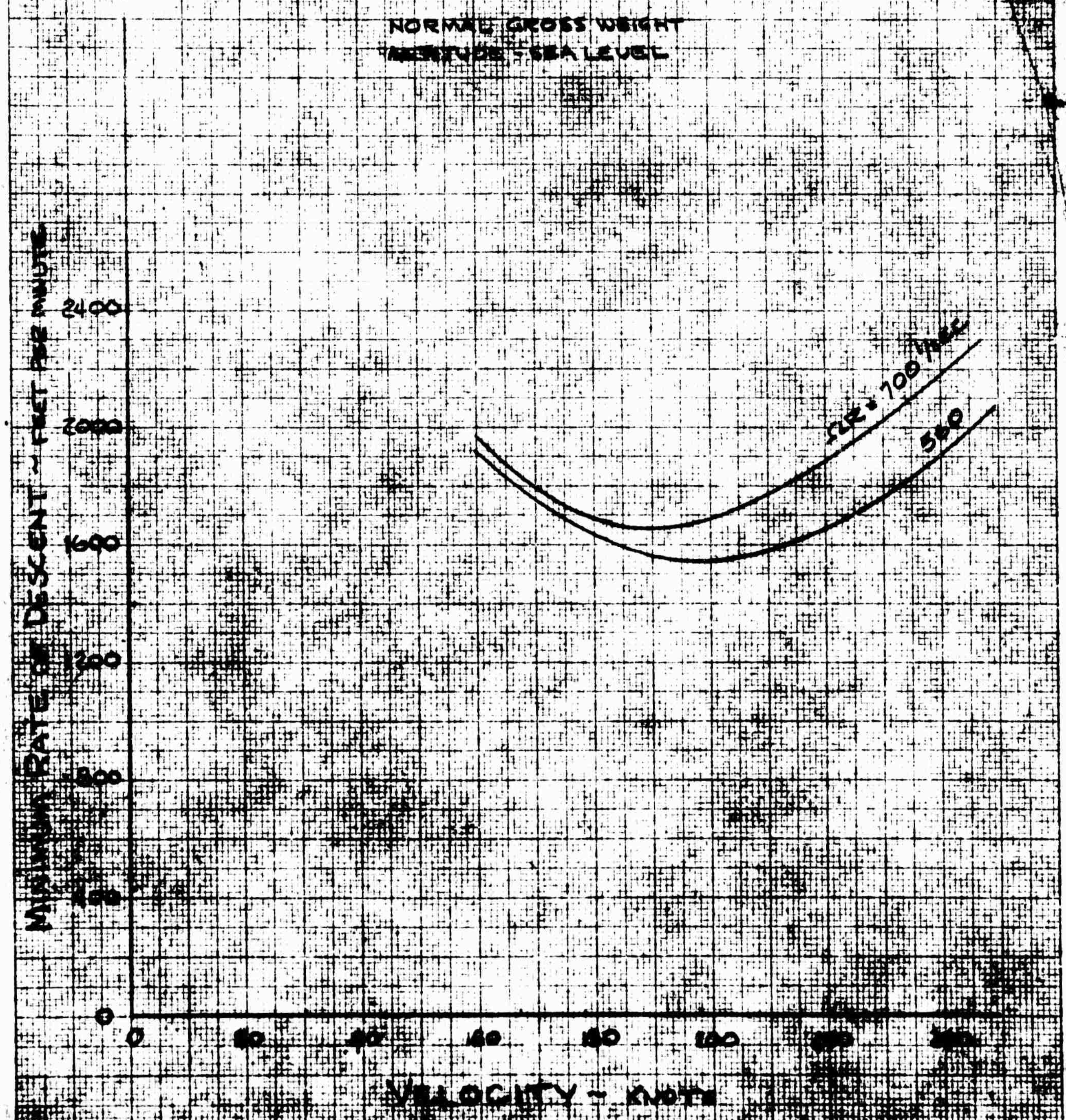

CONFIDENTIAL

20 December 1950

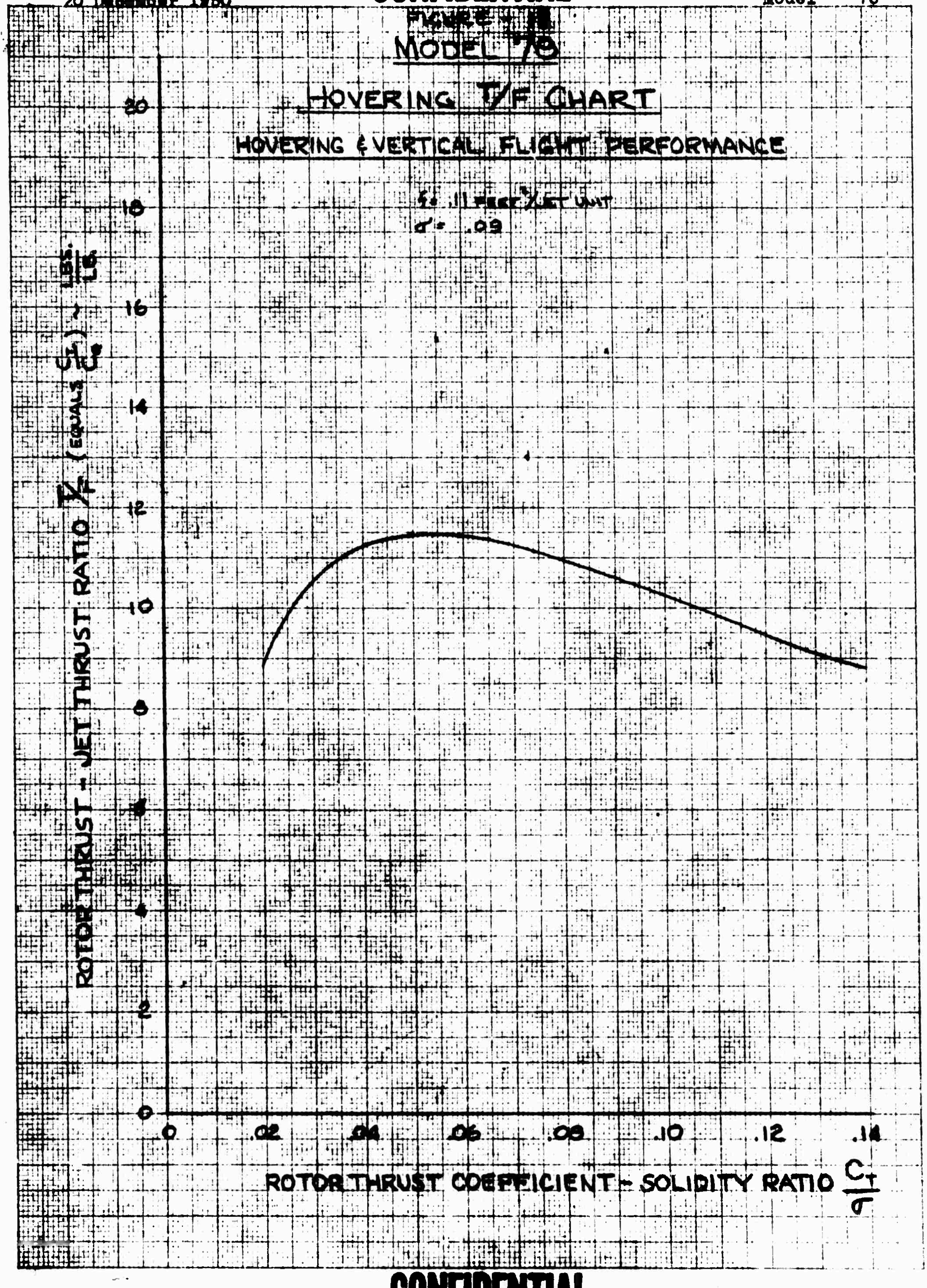

20 December 1950

CONFIDENTIAL

FIGURE - 16

MODEL 78

RATIO OF EXCESS POWER TO EFFECTIVE CLIMB POWER
vs
VERTICAL RATE OF CLIMB

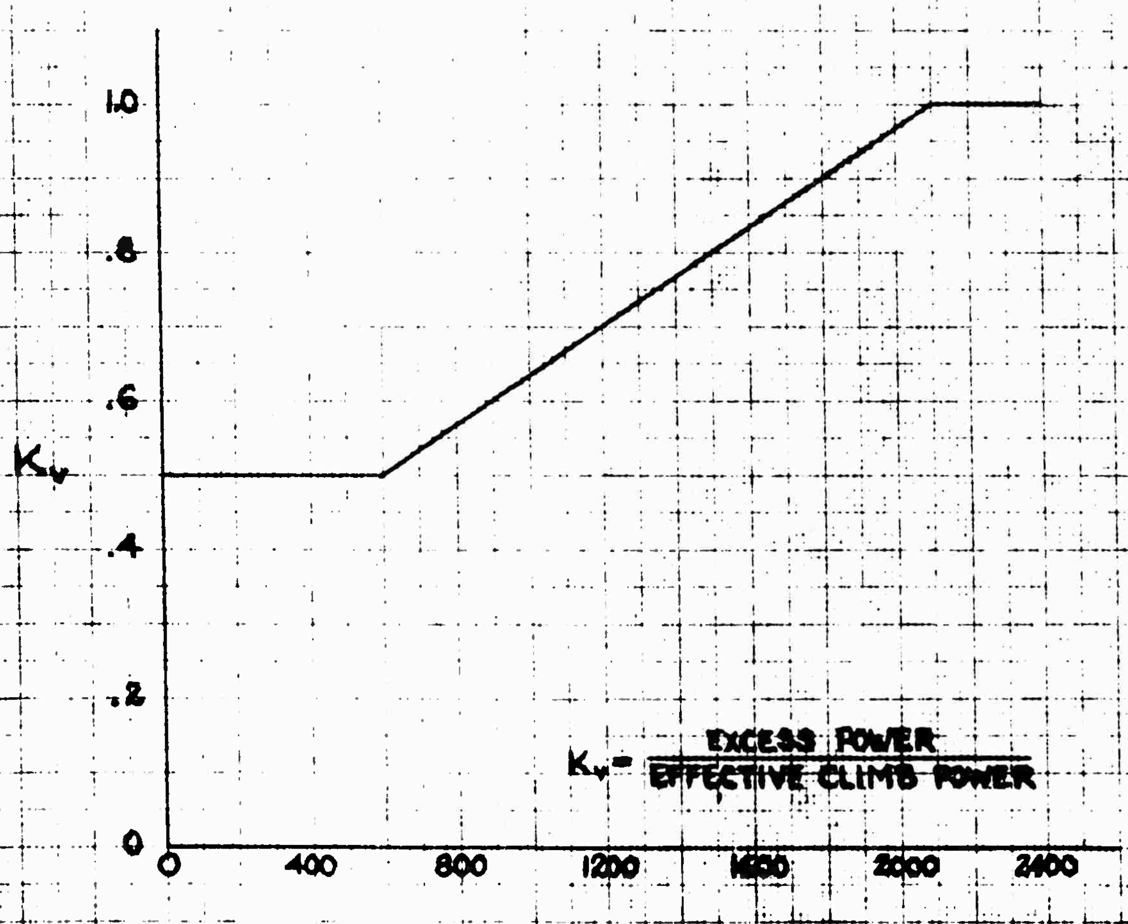

BASED ON NACA FLIGHT TEST RESULTS
REPORTED IN REFERENCE

CONFIDENTIAL

FIGURE -18

MODEL 78

C_T/σ AT STALL VS P/L OF ROTOR

REFERENCE - 9.8

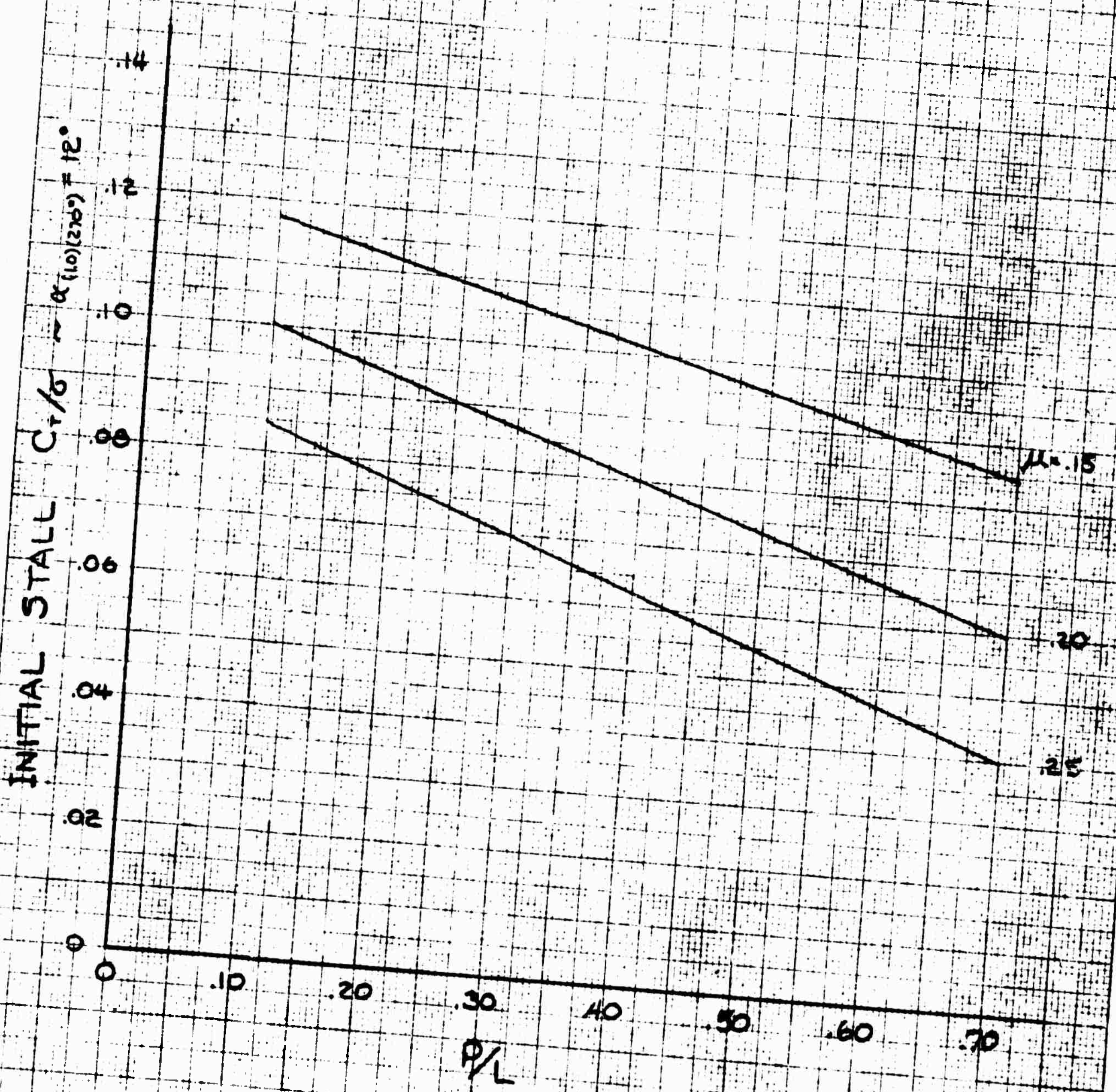

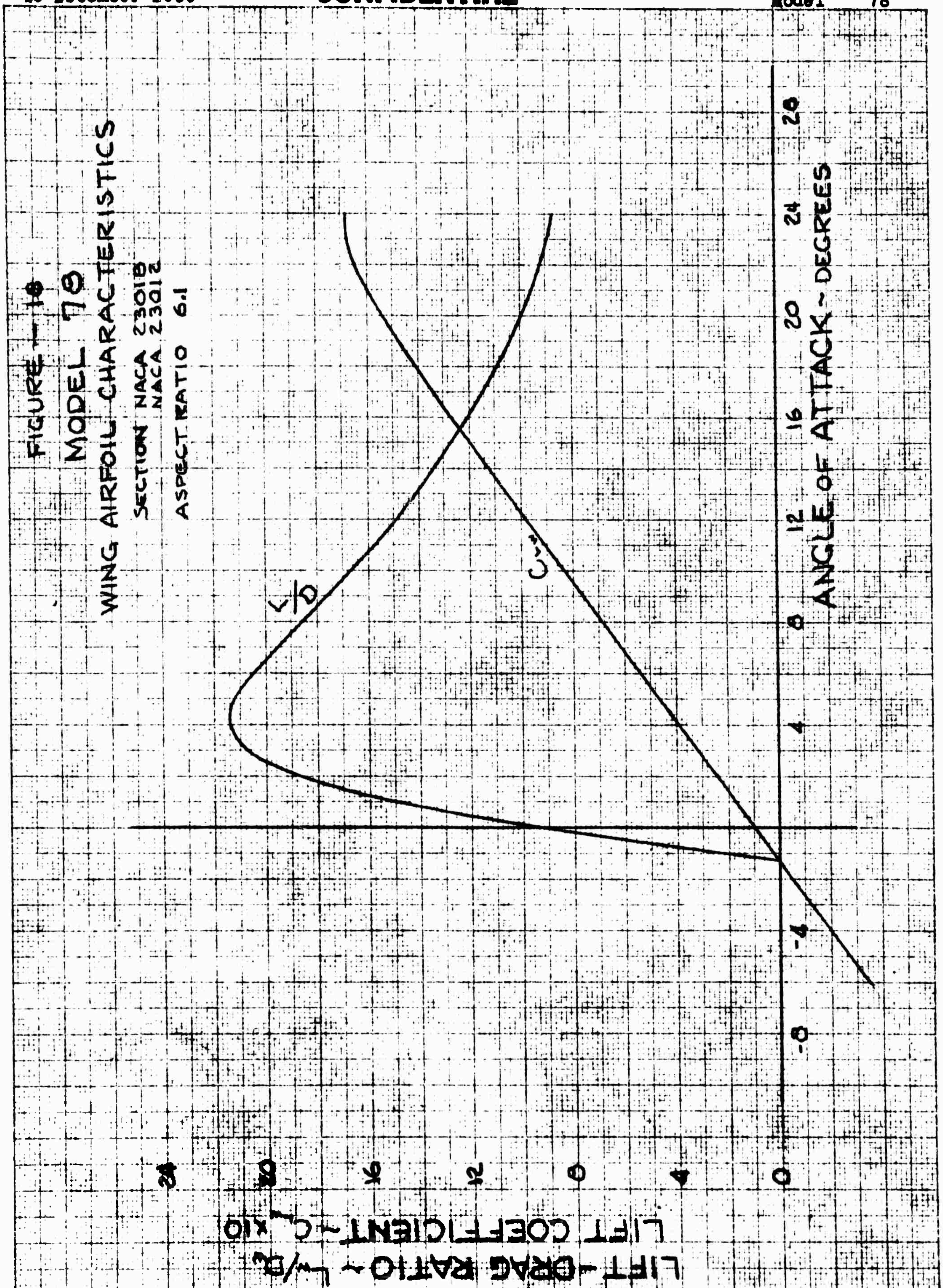
FIGURE 18
MODEL 78
WING AIRFOIL CHARACTERISTICS
SECTION NACA 23018
NACA 23012
ASPECT RATIO 6.1
L/D
C_L
ANGLE OF ATTACK ~ DEGREES
-8
-4
0
4
8
12
16
20
24
28
LIFT COEFFICIENT ~ C_L x10
LIFT-DRAG RATIO ~ L/D

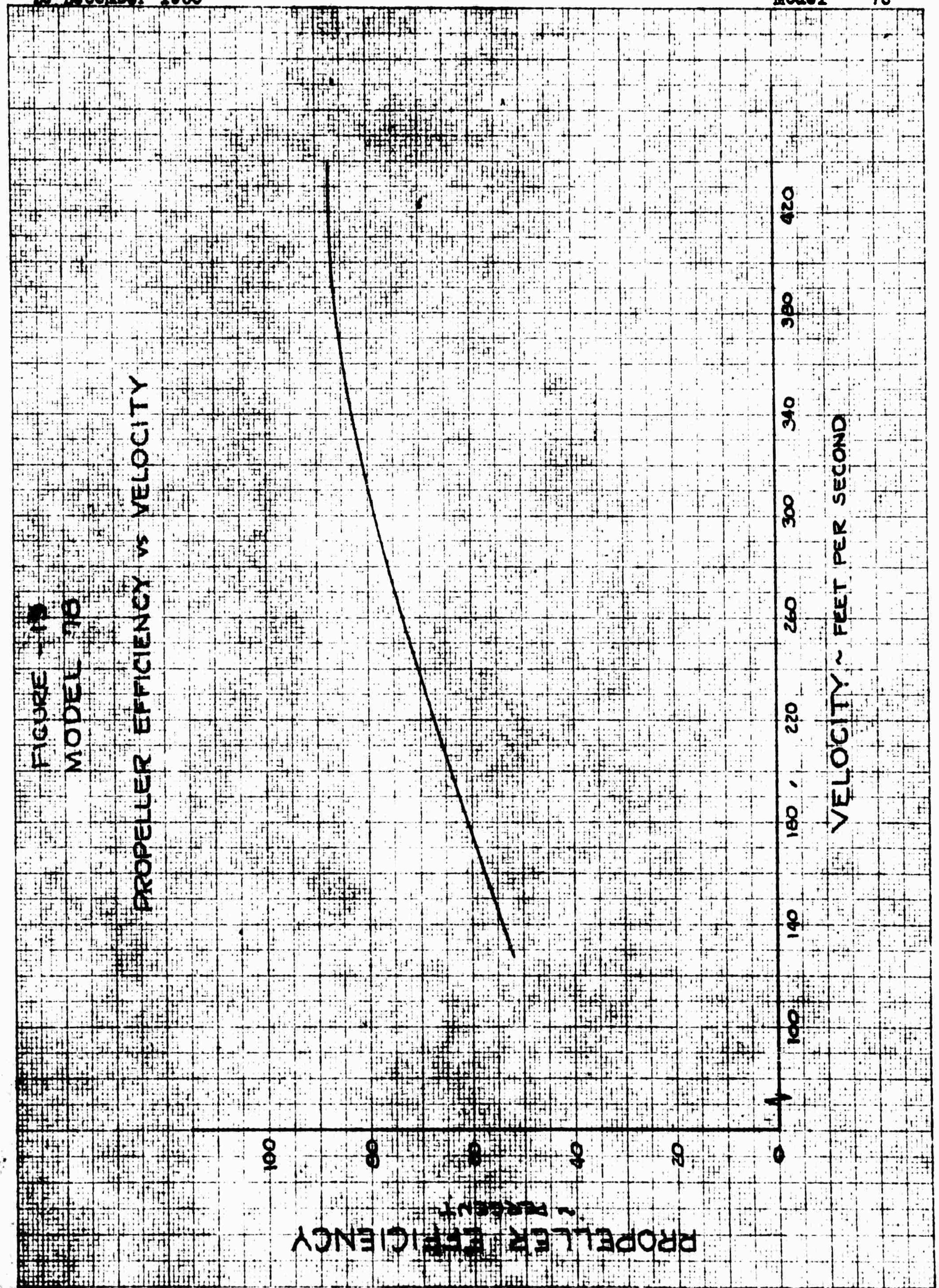
MODEL 78
PROPELLER EFFICIENCY vs VELOCITY
VELOCITY ~ FEET PER SECOND
100
140
180
220
260
300
340
380
420
PROPELLER EFFICIENCY ~ PERCENT
0
20
40
60
80
100

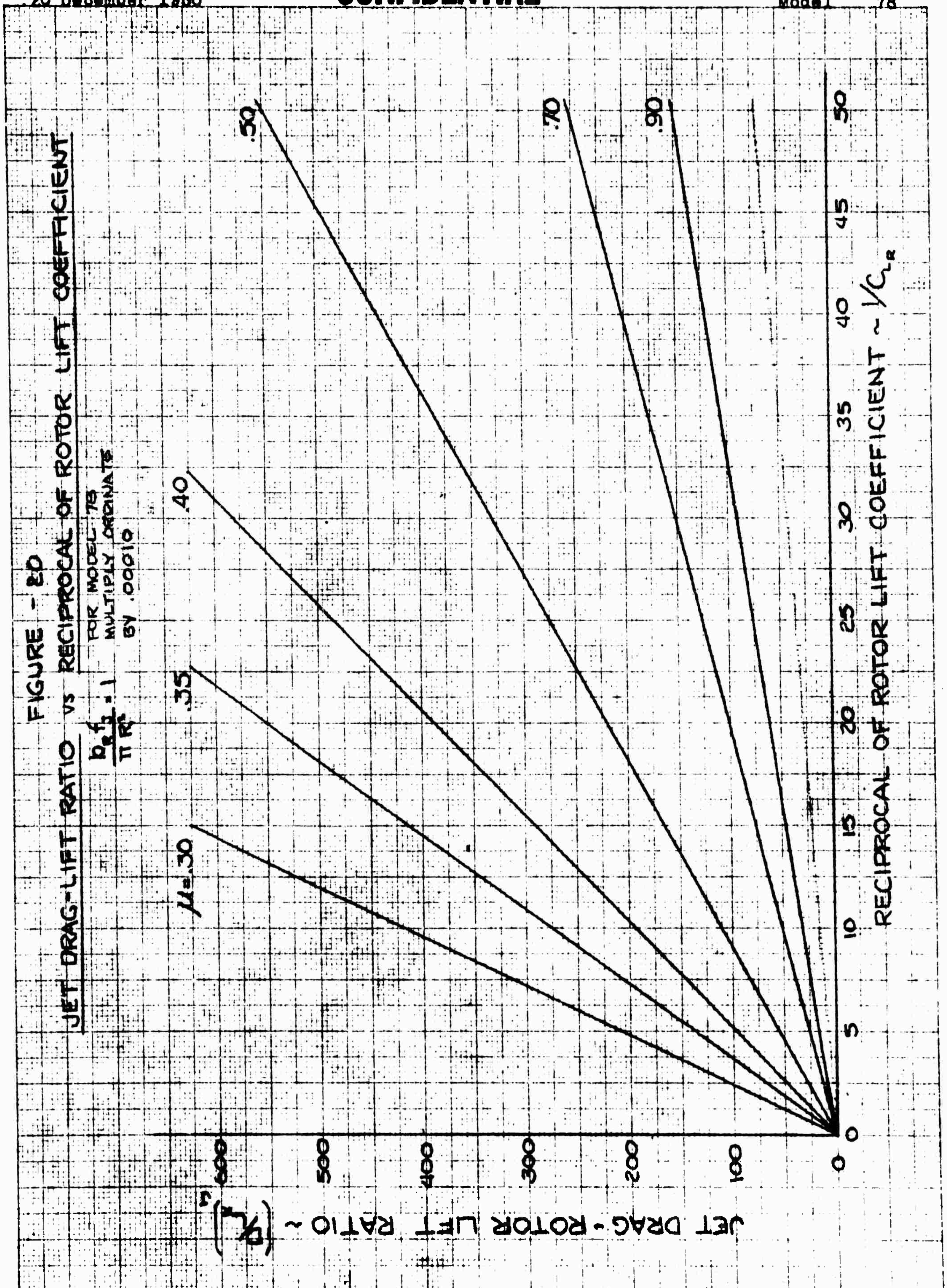

FIGURE - 20
JET DRAG-LIFT RATIO VS RECIPROCAL OF ROTOR LIFT COEFFICIENT

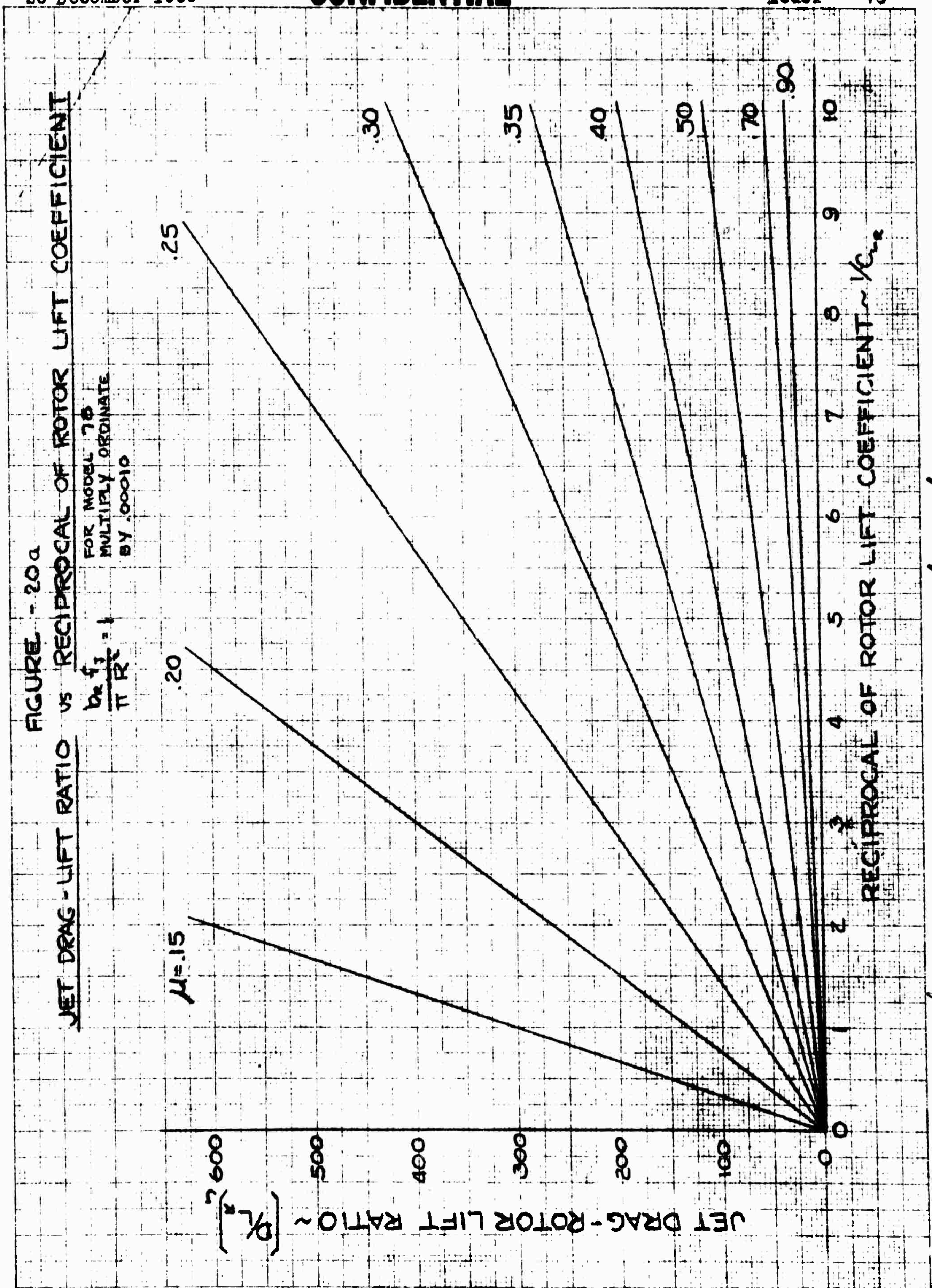

Same as pg 60 but scale is changed.

9. REFERENCES

9.1 BuAer confidential letter serial 09231, dated 5 September 1950.

9.2 "BuAer Specification for the Aerodynamic, Structural, and Power-Plant Requirements for Helicopters", NAVAER SR-189, effective 1 August 1950.

9.3 "Charts, Standard Aircraft Characteristics and Performance, Piloted Aircraft", MIL-C-5011, dated 20 January 1950.

9.4 Diehl, Walter S.: "Engineering Aerodynamics", Ronald Press Company, 1936.

9.5 Perkins, Cortland D. and Hage, Robert E.: "Airplane Performance, Stability, and Control", John Wiley and Sons, Inc., 1949.

9.6 Abbott, Ira A. and Greenberg, Harry: "Tests in the Variable-Density Wind Tunnel of the NACA 23012 Airfoil with Plain and Split Flaps", NACA T.R. 661, 1939.

9.7 Anderson, Raymond J.: "The Experimental and Calculated Characteristics of Twenty-two Tapered Wings", NACA T.R. 627, 1938.

9.8 Bailey, J. I., Jr. and Gustafson, J. B.: "Charts for Estimation of the Characteristics of a Helicopter Rotor in Forward Flight. I - Profile Drag-Lift Ratio for Untwisted Rectangular Blades", NACA ACR L4H07, 1944.

9.9 Brown, K. L.: "Model 78 Power Plant and Duct Analysis", MAC Engineering Report 1905, 1950.

9.10 Graha[illegible], [illegible] J., [illegible]itzber[illegible], [illegible], [illegible]lson, R. [illegible]: "A Systematic Investigation of Pressure Distributions at High Speeds over Five Representative NACA Low-Drag and Conventional Airfoil Sections", NACA T.R. 832, 1945.

9.11 Gustafson, J. [illegible], and [illegible]yers, [illegible], Jr.: "Stalling of Helicopter Blades", NACA T.N. 1083, 1946.

9.12 Gustafson, J. P. and [illegible]esson, Alfred: "Flight Tests of the Sikorsky HNS-1 (Army YR-4B) Helicopter. II - Hovering and Vertical Flight Performance with the Original and an Alternate Set of Main Rotor Blades, Including a Comparison with Hovering Performance Theory", NACA MR LSD09a, 1945.

9.13 Sissingh, G.: "Contribution to the Aerodynamics of Rotating [illegible]ing Aircraft", NACA TM [illegible]90.

9.14 Wheatley, J. [illegible]: "Wing Pressure Distribution and Rotor Blade Motion of an Autogiro as Determined in Flight", NACA T.R. 47[illegible], 1933.

9.15 Wheatley, J. B.: "The Influence of Wing Setting on the Wing Load and Rotor Speed of a PCA-2 Autogiro as Determined in Flight", NACA T.R. 523, 1935.

9.16 Wheatley, J. B. and Hood, [illegible] J.: "Full Scale Wind Tunnel Tests of a PCA-2 Autogiro Rotor", NACA T.R. 515.

9.17 Wheatley, J. B. and Bioletti, C.: "Wind Tunnel Tests of 10-Foot Diameter Autogiro Rotors", NACA T.R. 552.

9.18 McDonnell Aircraft Corporation Engineering letters submitted to the Office of Naval Research:

9.18.1 2136-701-1380, dated 6 July 1949

9.18.2 2136-701-1390, dated 26 August 1949

9.18.3 2136-701-1406, dated 14 November 1949

9.18.4 2136-701-1441, dated 13 January 1950

9.18.5 2136-701-14[illegible], dated 21 March 1950

9.18.6 2136-701-1544, dated 1[illegible] May 1950

9.18.7 2136-701-1[illegible]03, dated 14 July 1950

9.18.8 2136-701-1[illegible]26, dated 18 August 1950

9.18.9 2136-701-1644, dated 15 September 1950

9.18.10 2136-701-1667, dated 26 October 1950

9.18.11 2136-701-1675, dated 7 November 1950